Research Square

Preprints are preliminary reports that have not undergone peer review.
They should not be considered conclusive, used to inform clinical practice,
or referenced by the media as validated information.

Sustainable Toxic Basic Fuchsin Removal Using Activated Carbon and Adsorption Process Optimization: Factorial Design, Kinetics, Thermodynamic and Isotherm Analysis

Moussa ABBAS

moussaiap@gmail.com

UMBB: Universite M'Hamed Bougara Boumerdes

Zahia HARRACHE

UMBB: Universite M'Hamed Bougara Boumerdes

samir Chennouf

UMBB: Universite M'Hamed Bougara Boumerdes

Mohamed TRARI

USTHB: Universite des Sciences et de la Technologie Houari Boumediene

Research Article

Keywords: Activated Carbon, Box-Behenken, Isotherm, Reusability, Basic Fuchsin

Posted Date: April 24th, 2026

DOI: https://doi.org/10.21203/rs.3.rs-8609635/v1

License: This work is licensed under a Creative Commons Attribution 4.0 International License.
Read Full License

Version of Record: A version of this preprint was published at Applied Biochemistry and Biotechnology on August 3rd, 2026. See the published version at https://doi.org/10.1007/s12010-026-05842-3.

Sustainable Toxic Basic Fuchsin Removal Using Activated Carbon and Adsorption Process Optimization: Factorial Design, Kinetics, Thermodynamic and Isotherm Analysis

Moussa ABBAS [*, 1], Zahia HARRACHE [1], Samir CHENNOUF [1], Mohamed TRARI [2]

[1)] **Laboratory of Applied Chemistry and Materials (LabCAM), University of M'hamed Bougara of Boumerdes, Avenue de l'Indépendance Boumerdes, 35000, Algeria.**

[2)] **Laboratory of Storage and Valorization of Renewable Energies, Faculty of Chemistry (USTHB), BP 32-16111 Algiers, Algeria.**

*** (Corresponding author) E-mail moussa abbas : m.abbas@univ-boumerdes.dz, moussaiap@gmail.com**

Abstract

The increasing population has negatively impacted environmental water quality despite the strict policies implemented on wastewater treatment as the problem remains demanding. However, it is imperative to secure the environment for aquatic and human life. The physicochemical properties of AC were evaluated using several analytical techniques, including pH_{pzc}, BET, FTIR, and SEM-EDX analysis. The Box-Behnken design was used to optimize three important parameters including the initial concentration of Basic Fuchsin (BF) (100-200 mg/L), pH (6-10) and the dose of activated carbon CA (0.1-0.5 g) on the removal of BF on AC. The experimental data obtained were discussed by analysis of variance (ANOVA) and tensions to a second-order polynomial equation using multiple regression analysis, the optimal conditions obtained by the exploitation of 3D contours and surfaces are: (initial concentration of BF: 178.074 mg/L, pH of the initial solution: 6.78 and the dose of CA: 0.3837 g at temperature: 25 °C). Different isotherm models were used to fit the experimental data, the results indicate that the Langmuir model offers the best correlation; the maximum adsorption capacities obtained are respectively 34.482, 66.667 and 93.467 mg/g at temperatures 20, 30 and 40 °C. Kinetic modeling showed that adsorption obeys the pseudo-second-order kinetic model (R^2 = 0.999). The effect of temperature on adsorption isotherms allowed obtaining the following thermodynamic functions: The negative values of free energy ΔG° (-11.455 to - 6.415 kJ/mol) and a positive enthalpy ΔH° (67.421 kJ/mol), confirming the spontaneous and endothermic nature of BF adsorption on CA. The positive entropy ΔS° (252 J/mol.K) shows an accumulated random character of the solid-liquid interface during adsorption. The adsorption of the FB dye onto the AC surface can be explained by several possible interactions including π-π stacking, electrostatic forces, pores filling, and hydrogen bonding. The photochemical study reveals that CA is harmful to germination and soil and that BF positively influences plant germination.

Keywords: Activated Carbon, Box-Behenken, Isotherm, Reusability, Basic Fuchsin.

1. Introduction

With increasing population and industrialization, waste generation has surged, making wastewater a major concern. Industrial effluent from pharmaceuticals, paper and pulp, chemicals, refineries, textiles, and food etc. contain toxic compounds detrimental to plant and animal life. Dye-laden wastewater, particularly from textile, leather, and tanning industries, significantly contributes to environmental pollution, affecting human health and surroundings. The dyes composed of complex organic compounds with azo bonds and polyaromatic rings are toxic and difficult to degrade. If they are directly discharged into the river, they will

have a great negative impact on the environment due to hindering the self-purification of the water body and poisoning the microorganisms and fish. Therefore, it is essential to remove dyes from wastewater before discharging in order to avoid pollution environment. Dyes are one of the largest water pollutants worldwide **[1]**. On a large scale, dyes enter water and wastewater either directly from the dye manufacturing industry or from the finishing steps in coloring other industrial products such as textiles, cosmetics, leather, food, and paper **[2]**. In addition to their effect on increasing the biochemical oxygen demand by preventing light penetration in aquatic systems which is essential for photosynthesis, most synthetic dyes are toxic **[3]**, mutagenic, and carcinogenic **[4]** and cause detrimental effects on the water environment if not removed from effluents before entering the ecosystem. Basic Fuchsin (BF) is one such dye which is carcinogenic and mutagenic in nature. BF is a dye which finds wide application in textile, cosmetic and pharmaceutical industries. It is also used as a staining agent in medical laboratories. Wastewater containing FB can thus be released into environment from these industries and laboratories. The allowable limit of FB in wastewater varies by regions and countries and it is highly dependent on local legislation. As per EPA, the general colourant limit is < 1 mg/L in wastewater to avoid any harmful effects to the environment. Basic Fuchsin is a tri-amino, tri-phenyl methane dye with molecular formula $C_{20}H_{20}ClN_3$. It is a mixture of three dyes Para rosaniline, Rosaniline, and Magenta II and thus known as Magenta II **[5].** It is one of those rare dyes that is inflammable in nature. It is widely used as coloring agent for textile and leather materials. It is also used to stain collagen, muscle, mitochondria, and tubercle bacillus **[6]**. It possesses anesthetic, bactericidal, and fungicidal properties **[7, 8].** The physical contact with the dye may cause severe eye and skin irritation. Its ingestion may cause gastrointestinal irritation with nausea, vomiting, and diarrhea and the inhalation of the dye causes irritation to the respiratory tract **[9]**, Inhalation or ingestion may also cause damage to the organs such as blood, liver, spleen, and thyroid **[10]**. Repeated exposure to the dye may affect the nervous system with headache, dizziness, lethargy, and muscle contraction. In humans and animals, its toxicity includes carcinogenic and mutagenic effects **[11].** Thus, keeping the toxicity of the dye in view, there is a need to develop effective methods for its removal from the wastewater. Formerly, several conventional methods have been tried to remove various dyes from industrial effluents **[12]**. The literature is rich with techniques and procedures for removing chemical dyes from aqueous media. Various authors have evaluated supplies of animal or vegetable origin **[13]** for the decontamination of aqueous media by chemical dyes. Adsorption, particularly using carbon adsorbents, is an alternative for removing pollutants from wastewater. The adsorbent properties of AC have been shown to depend on their surface area, functional groups, their Π- electron system capable of forming strong bonds with various pollutants, and their porous structure. Furthermore, stability, concentration, and overall quality of the carbon material dispersion are also critical to the adsorption process, especially for the removal of organic dyes such as basic fuchsine and other popular pharmaceutical compounds. Various biological, chemical, and physical methods such as biodegradation, Fenton-biological treatment scheme, chemical oxidation, ozonolysis, filtration, ionic exchange, photo degradation, membrane technologies, coagulation/flocculation, and adsorption were tested for removing wastewater dye **[14-17]**. Among these, adsorption is one of the most environmentally friendly, easy to operate, and cost effective method. The adsorbent material plays a crucial role in the process, requiring specific structural characteristics such as appropriate pore size, high specific surface area, good selectivity, thermal an chemical stability and low cost. Given the numerous parameters influencing optimal performance, enhancing AC has become a key focus of recent research. Response Surface Methodology (RSM) is a statistical approach commonly used for efficient multivariable optimization and process modeling **[18]**. A commonly preferred method in Response Surface Methodology (RSM) is the Box-Behnken Design (BBD). This approach effectively builds predictive mathematical models that link input variables to corresponding responses while reducing the number of experimental trials needed. It also facilitates a comprehensive examination of interaction effects among the variables. Additionally, three-

dimensional (3D) plots are utilized to visualize the influence of parameters, and Analysis of Variance (ANOVA) is employed to confirm the accuracy and significance of the results **[19-21]**. The characterization of the adsorbent is presented and the removal rate kinetics, thermodynamics and isotherms for Basic Fuchsin adsorption onto AC were also studied.

2. Materials and Methods

Determination of the point of zero charge

The Zero Point Charge pHzpc of the adsorbent, which corresponds to zero surface charge, is obtained using the procedure reported elsewhere **[22].** The pH of each solution was measured by using a microprocessor-based pH meter; Model HI 8424 (M/s Henna Instruments, Italy) and absorbance measurements were carried out on a Model 117 UV/VIS spectrophotometer (M/s Systronics, Ahmed abad, India) over the wavelength range 200-500 nm. Measurements of the residual concentrations were obtained by linear interpolation from a previously established calibration curve.

Analyses of the AC Surface Morphology

Scanning electron microscopy (SEM) images were obtained on a Philips-FEI model Quanta 200. The samples were held with carbon adhesive tape on aluminum sample holder, and then coated with a gold layer using a sputter coater (Bal-Tec, SCD-050 model, Balzers, Liechtenstein), subsequently, examined with an operating voltage of 20 kV and a current of 30 mA. The morphology, arrangement of the cavities and their dimensions in the prepared AC, before and after BF adsorption was examined.

Analyses of the AC Surface Chemical

The FT-IR spectroscopywas used to identify the characteristic functional groups on the AC surface before and after adsorption, ~ 5 mg of adsorbent were mixed with dry KBr and compacted under a pressure of 4500 psi to form thin disc. The spectra were plotted with a Perkin Elmer 2000 infrared spectrometer between 400 and 4000 cm^{-1} for 16 times to increase the signal to noise ratio

Specific surface area

The N_2 adsorption–desorption isotherms of samples were recorded at −196°C using Bel Sorp-Max (Bel Japan Inc.). Before analysis, the sample (ca. 1000 mg) was degassed at 350°C for 5 h. The surface area was calculated using the Brunauer–Emmett–Teller (BET) equation.

Basic Fushcin adsorbate

The basic Fuchsin (BF, 98% purity), used in this study, was supplied by Sigma-Aldrich Company, BF was used as supplied without any further purification; the stock solution (1000 mg/L) was prepared and the BF solutions used for the experiments were prepared by dilution. The concentration of BF was titrated at the maximal wave length (λ_{max} = 542 nm), using UV–Visible spectrophotometer (UV 2300), by linear interpolation of the calibration graph.

Adsorption isotherms and kinetics Experiment

The kinetic study was conducted to evaluate the adsorption rate and to determine the required contact time for equilibrium. In this work, three kinetic models were applied to describe the adsorption process: the

pseudo-first-order, pseudo-second-order, Elovich and intra-particle diffusion models. To further analyze the adsorption mechanism at equilibrium, the experimental data were fitted to the Langmuir, Freundlich, and Temkin isotherm models. These isotherms provide insights into the adsorption capacity, surface heterogeneity, and adsorbate-adsorbent interactions.

Box-Behnken experimental design

The batch balancing method was applied for the optimization process according to the Box-Behnken design matrix *Expert 12 software*. The most significant variables of BF adsorption were considered, pH (X_1), adsorbent dose (X_2), and concentration (X_3), in order to study their impact on BF elimination. The low, center and high levels of each variable are denoted by (-1, 0 and 1), as shown in **Table.1**. The response results were evaluated by a second-order polynomial, including individual, square, and interaction terms for each variable and the secondary response model is as follows **[23].**

$$R(\%) = a_o + \sum_{i=1}^{K} a_i x_i + \sum_{i=1}^{k} \sum_{j=1}^{k} a_{ij} x_i x_j + \sum_{i=1}^{k} a_{ii} x^2_i \qquad (1)$$

Where R (%) is the predicted response which actually represents the removal efficiency of BF adsorbed a_0 a constant coefficient, x_i and x_j variables. a_i, a_{ii} and a_{ij} are the interaction coefficients for linear, quadratic and second order terms, respectively.

The experimental matrix of CCD was proposed by *Expert Design 12* which was also used to determine the regression analysis of designed model and graphical analysis of each response. The total number of experiments calculated using the following equation:

$$N = K^2 + k + Cp \qquad (2)$$

k =3, the number of independent variables, Cp =3, the number of experiment repeated at center points a total of experiments (N=15) were designed using the RSM method and optimized by a central composite design **Table 2**. For this, 50 mL of BF aqueous solution with different pH, initial concentration, temperature and adsorbent dose was placed in a 125 mL glass bottle. The mixture was agitated at 200 rpm and at fixed contact time (30 min) that was obtained from kinetic study. The solution was then filtered and the residual BF ion concentration analyzed. The amount qt (mg/g) yield R (%) of BF adsorbed by adsorbent (q_t) was calculated from the relations:

$$q_t = \frac{(C_0 - C_t) \cdot V}{m} \qquad (3)$$

$$R_t(\%) = \frac{(C_0 - C_t).100}{C_0} \qquad (4)$$

Where C_o is the initial BF concentration and C_t the concentrations (mg/L) at time t, V is the volume of solution (L) and m is the mass of AC (g).

Modeling and Statistical Analysis

The adsorption experiments were performed in triplicate, and the average data values were used for the construction of graphs. Data analysis involved the application of one-way analysis of variance (*ANOVA*) using *Origin Pro 08*. Statistical significance was considered at $p < 0.05$. Additionally, the fitting models with the experimental data were tested using error functions for significant results.

To confirm the correlation a statistical error calculation is essential, among the most used error functions are the following. Due to the inherent bias resulting from linearization of the isotherm model and kinetic model, for non-linear regression, the determination coefficient (R^2) is insufficient for evaluating the fit goodness,

thus, the application of error models, Chi-Squares (X^2) test equation is used as criteria for the quality of fitting.

$$X^2 = \sum_1^N \frac{(q_{e,exp} - q_{e,cal})^2}{q_{e,cal}} \quad (5)$$

Where, $q_{e(exp)}$ (mg/g) is the experimental value of uptake, $q_{e(cal)}$ the calculated value of uptake using a model (mg/g) and N the number of observations in the experiment (the number of data points). The smaller X^2 value indicates the better curve fitting.

3. Results and Discussions

Adsorbent characterization

To determine the areas of predominant charge distribution on the surface of the AC adsorbent, briefly, 20 mL of KNO_3 (>99%) solutions (0.01 M) were placed in closed conical flasks and the pH was adjusted between 2 and 14 with HCl (37%) or NaOH (97%) solution. 0.1 g of adsorbent was added at each solution and the final pH was measured after 24h under stirring at ambient temperature; pHzpc (7.50) corresponds to the intersection of the final pH and pH curves **(Figure.1).**

pH is a crucial parameter in the adsorption process. pH_{PZC} was used to determine the pH at which the net adsorbent surface charge is zero. It is obvious that the percentage of elimination of BF increases with the increase of the pH of the medium. The effect of pH on the adsorption by AC can be explained on the basis of pH_{PZC}, for which the adsorbent surface is neutral. The surface charge of the AC is positive when the medium pH is under pH_{PZC} and negative for higher pH than pH_{PZC} of AC is 7.50. This behavior may be due to the fact that the AC surface is negatively charged at pH > pH_{PZC}, which favors the adsorption of cationic dyes BF. Conversely, for pH values < pH_{PZC}, the surface of AC is positive, and thus it repels the BF molecules. As pH increases, the number of negatively charged sites increases and improves the BF adsorption by electrostatic attractions; Similar experimental details have been reported by Abbas et al. **[24]**.

In order to determine the specific surface area of the studied compound, nitrogen sorption was measured on a Bel Sorp-Max (Bel Japan Inc.). The collected data was subjected to (BET) treatment. The volume of mesopores as well as micropores has been obtained through the application of the t-Plot methods to the nitrogen adsorption data. The surface properties of the AC were determined from the N_2 gas adsorption-desorption isotherms at 77 K **(Figure .2)**. The BET surface area (BET), BJH pore volume, and mean pore diameter were estimated at 836.575 $m^2 g^{-1}$, 0.05275 $cm^3 g^{-1}$, and 12.6114 Å, respectively before adsorption and they decrease after adsorption to 762.655 $m^2 g^{-1}$, 0.5373 $cm^3 g^{-1}$, 14.0897 Å ,which confirms that the cavities are occupied by BF. The large surface area provides numerous active sites for dye adsorption, while the mesoporous channels facilitate efficient diffusion of MB and MO molecules into the adsorbent. The hysteresis, where the desorption isotherm appears above the adsorption isotherm, becomes noticeable at a low relative pressure (p/p_o<0.4) due to the low rate of diffusion in the inner pores.

The Scanning Electron Microscope (SEM) micrographs of AC before and after adsorption are shown in **(Figure.3)**. The SEM analysis of the adsorbent revealed a highly porous and rough surface with irregular cavities, which are favorable for dye adsorption. Before adsorption, the presence of cracks and channels indicated abundant active sites. After BF adsorption, the pores appeared partially filled and smoother regions became visible, suggesting partial surface coverage by dye molecules. In contrast, after BF adsorption, significant pore blocking and a noticeable dye layer deposition were observed, indicating stronger surface coverage. These morphological changes confirm successful dye attachment onto the adsorbent and align with the FTIR findings, demonstrating the efficiency of the adsorbent in capturing dye.

After adsorption, the AC surface became smoother with a roughness was considerably reduced with less visible pores, and this indicates a clear adsorption on both the surface and within pores. The images also reveal that the exterior surfaces of the AC are filled with more or less homogeneous cavities of different sizes and shapes. These cavities differ from carbon to carbon in the reaction of the activating agent. These cavities are the external pores which represent the main channels for accessing to the internal surface of the activated carbon. The higher magnification clearly shows that the adsorbent surface contains a considerable number of pores with a high probability that BF ions are adsorbed.

The FT-IR spectra were carried out to elucidate the chemical structure of the film and **Figure.4** which represents the different bands detected in the spectrum of the adsorbent AC before and after the dyes adsorption the distinct four bands (466.67; 1453.56, 1786.48, 2121.69, 2354.7 cm^{-1}) are attributed to C-Br C-I, C=C (aromatic) $-CH_2$ shear, C-H deformation, C=C=C, C-C, C-N, C-H bending; C-C, and C=C, C-N, indicating the presence of pollutant binding sites.

Experimental design analysis by Box Behnken design

The obtained for the comparison of experimental yields and those calculated by the mathematical model during the eliminations of BF on activated carbon are shown in Figure.5 and Table.2 to confirm the correlation of the results, a plot of the $R_{exp} = f(R_{pred})$ curve is carried out, the latter clearly shows that the experimental results and those deduced by the model are in perfect correlation ($R^2 = 0.984$). *P*-values less than 0.05 indicate significant model terms. In this case X_1, X_2, X_3, X_1^2 are also significant model terms while the opposite effect occurs for values greater than 0.1000. If there are many insignificant model terms, model reduction may improve the model.

The empirical relationship between the response and the independent variables of the process was obtained based on the results, given by a second-order polynomial:

$$R_{BF}(\%) = 88.03 + 1.47\,X_1 + 5.26\,X_2 + 0.1800\,X_3 - 2.68\,X_1^2 + 4.08\,X_2^2 + 1.97\,X_3^2 + 0.6025\,X_1X_2 - 2.33\,X_1X_3 - 1.19\,X_2X_3$$

Where R is the percentage removal of BF; X_1, X_2, and X_3 are the coded values of pH, activated carbon dose (g/L), and initial concentration Co (mg/L), respectively. The results of the analysis of variance, analyzed using *Expert Pro 12* for the adsorption study, are shown in Table.3.

The lack-of-fit F-value of 31.10 indicates that the model is significant. There is only a 3.13% chance that a lack-of-fit F-value this large could occur due to noise. The A_{deq} Precision measures the signal-to-noise ratio. A ratio greater than 4 is desirable. A ratio of 9.101 indicates an adequate signal. This model can be used to explore the design space.

P-values less than 0.0500 indicate that the model terms are significant. In this case, X_1^2, X_2 and X_2^2 are significant terms. The values greater than 0.1000 indicate that the model terms are not significant. In the ANOVA results, it is noted that the linear parameters X_1 and X_2, the interaction parameters X_1X_2, X_1X_3, X_2X_3, and the quadratic parameter X_3^2 are not significant. The resulting modified BBD model is expressed by the equation:

$$R_{BF}(\%) = 88.03 + 5.26\,X_2 - 2.68\,X_1^2 + 4.08\,X_2^2$$

The equation in terms of coded factors can be used to predict the response for given levels of each factor. By default, high levels of the factors are coded as +1 and low levels as -1. The coded equation is useful for

identifying the relative impact of the factors by comparing the factor coefficients. The equation in terms of actual factors can be used to predict the response for given levels of each factor.

Optimization by RSM and with desirability function

Expert design 12 to study graphically the interactions by 2D contours, which are suitable for studying binary interactions of factors. The contour plots of the second-order polynomial equation within two independent variables (adsorbent dose and C_o, pH concentration and C_o, pH and adsorbent dose), while the other values are kept fixed. **Figure.6** delivers the information on their connections and relationships; it can also include the main factor and the interaction impacts of these two independent factors **[25, 26]**.

Examination of the 2D curves of the binary variables of the BF **Figure.6** allows the determination of the following optimal conditions to achieve the maximum dye removal efficiencies. (D = 0.30 g, pH = 8.0, C = 150 ppm).

By the exploitation of 3D representation reveals **Figure.6** that the results obtained by the 2D courses present a correlation of results which confirms the validity of the quadratic model and allows the determination of the following optimal conditions to achieve the maximum dye removal efficiencies (Dose = 0.30 g, pH = 8.0, C = 150 ppm).

The desirability function approach is a technique for simultaneously knowing the optimal parameters of input variables that can determine the optimal performance levels for one or more responses and takes place in two stages:

i) Finding the levels of the independent variables that simultaneously produce the most desirable predicted responses on the dependent variables
ii) Maximize the overall desirability with respect to the controllable factors. The desirability function approach was initially introduced by Harrington **[27]**.

Depending on whether a particular response y_i is to be maximized, minimized or assigned a target value, the different desirability functions d_i (y_i) used are those proposed by Derringer **[28]**. In order to compare these results obtained, a study by desirability function (d=0.8) was carried out **Figure.7**, the maximum BF removal proposed by the *Expert design 12* is reached under the optimum conditions: pH = 6.7847, C = 178.074 ppm and dose D = 0.3836 g corresponding to the maximum BF removal efficiency R = (98.35 ± 0.75) %.

Perturbation plots Additionally, **Figure.8.** Displays perturbation curves for all the responses based on different parameter conditions in this study A (pH), B (concentration) and C (adsorbent dosage). The slope of each curve indicates the sensitivity of the responses to the respective factors. We notice from the curves that the slope of pH is greater than concentration indicating that they have the most significant impact on all the responses. It self greater than adsorbent dose.

Adsorption Isotherm study

The amount of adsorbate per unit mass of adsorbent at equilibrium, q_e (mg/g) and the adsorbate equilibrium concentration, C_e (mg/L) allow plotting the adsorption isotherm, q_e versus C_e, mathematical models were used to describe and characterize the adsorption processes. The experimental data were fitted to four common isotherm models which describes the solid-liquid sorption of BF onto AC.

Langmuir model **[29]** postulates the occurrence of monolayer adsorption onto a fixed number of localized sites on an adsorbent surface. The model assumes that a given adsorbent surface is composed of sites

equivalent in their enthalpies but with no further motion of the adsorbed molecules on the surface, and no interactions between the adsorbed molecules; the linear expression is given by**:**

$$\frac{1}{q_e} = \frac{1}{q_m} + \frac{1}{q_m.K_L.C_e} \quad (6)$$

$$R_L = \frac{1}{(1+K_L C_0)} \quad (7)$$

The type of isotherm is indicated by the coefficient R_L value: (R_L= 0): Adsorption is irreversible, (0 <R_L<1): Adsorption is favourable, (R_L=1): Adsorption is linear, (R_L>1): Adsorption is unfavourable.

Freundlich's model **[30]** is based on the formation of multilayer's of adsorbed species on a heterogeneous surface. The adsorbent surface site enthalpies have a logarithmic distribution, where the energy sites with high affinity for the adsorbate are occupied first, followed by sites of lower energy. The sorption process is summed over all sites and the linear expression of the Freundlich model is given by:

$$\ln q_e = \ln K_F + \frac{1}{n}\ln Ce \quad (8)$$

K_F (L/g) and *n* are constants, related respectively to the capacity of adsorption and favorability of adsorption extracted from the plot lnq_e versus lnC_e. When *n* is between 2 and 10, favorable adsorption is expected, Values of adsorption intensity (1/n) less than 1 indicate stronger bonding between the adsorbate and the adsorbent.

Similar to Freundlich's model, Temkin's **[31]** postulates the heterogeneity of an adsorbent surface, whose distribution of adsorption energy is linear; the non-linear form is given by:

$$q_e = B_T \ln C_e + B_T \ln A \quad (9)$$

$$B_T = \frac{q_m.R.T}{\Delta Q} \quad (10)$$

$\Delta Q(J/mol)$ is the adsorption energy change and q_{max} (mg/g) the maximum adsorption capacity. The adsorption data were analyzed according to the linear plot q_e versus lnC_e, enabling to calculate the constants A_T and B_T. Temkin isotherm helps to predict the heat of adsorption and the positive value of Temkin constant supports the exothermic adsorption

Elovich model **[32]** assumes that the number of adsorption sites augments exponentially with the adsorption, thus implying a multilayer adsorption:

$$\ln \frac{q_e}{C_e} = \ln(K_E.q_m) - \frac{q_e}{q_m} \quad (11)$$

Where K_E (L/mg) is a constant, q_{max} (mg/g) the maximum adsorption capacity, q_e (mg/g) the adsorption capacity at equilibrium and C_e (g/L) the concentration of the adsorbate at equilibrium. Both the constants K_E and q_e are calculated from the plot of $\ln(q_e/C_e)$ versus q_e.

The parameters of the models obtained after modeling the isotherms at different temperatures are summarized in **Table.4**. It is noted that the experimental isotherms are of type L, monolayer adsorption, and the Langmuir model exhibits the best correlation **Figures.9.** This is confirmed by the coefficient of determination R^2 = 0.99 and the low value of the statistical error X^2.

The maximum adsorption capacities obtained are respectively 34.482, 66.667 and 93.467 mg/g at temperatures 20, 30 and 40 °C respectively. Noted that R_L indicates the type of isotherm: Irreversible (R_L= 0), Favourable (0<R_L<1), Linear (R_L=1) or Unfavourable (R_L> 1).

In our case, the R_L values are smaller than 1, thus confirming that the adsorption is well described by the Langmuir isotherm frequently suggests one of the following three main hypotheses:

In a first step and over a short period, it is assumed that BF is transported to the external surface of the adsorbent by film diffusion at a high velocity.

After saturation, BF molecules penetrate into the adsorbent by intraparticle diffusion through the pores and diffusion to the internal surface until equilibrium is established.

Adsorption kinetic study

Influence of contact time and BF concentration of on the adsorption capacity

The MB concentrations and the mass of the adsorbent are important factors for the adsorption. To demonstrate the effect of the initial dye concentration (C_o) on the adsorption, experiments were performed at different BF concentrations. We performed the experiments for C_o valises (100-200 mg/L) and a mass of the AC of 5 g/L. The temperature is maintained constant at 25 °C and the mixture is stirred at 200 rpm. The samples are taken at regular time intervals, vigorously centrifuged for 10 min and finally analyzed by UV-visible spectrophotometer. We notice from **Figure.10** a very rapid adsorption, since a saturation level is reached after only 30 min; the latter indicates the formation of a monolayer. Note that the adsorption capacity increases with augmenting the BF concentration; this is due to the fact that the diffusion of the MB molecules from the solution to the surface of the adsorbent is accelerated by the increase in the dye concentration; similar result was already obtained for the adsorption of BF onto AC **[33].** With raising the initial MB concentration (100 to 200 mg/L), BF removal efficiency decreases from (42 to 98 mg/g) and we can deduce that the adsorption of BF onto AC is done in three stages:

i) *In range (0-10 min)* fast adsorption of BF due to the presence of free sites on the adsorbent surface which translates the linear increase of the adsorption capacity over time.

ii) *In range (10-20 min)* reduction of the adsorption rate, reflected by a small increase in the adsorption capacity attributed to the decrease in the quantity of BF in solution and the number of available unoccupied sites**.**

iii) *In range (20-35 min)* stability of the adsorption capacity is observed, due to the total occupation of adsorption sites: the establishment of the stable level therefore reflects this stage. The adsorption capacity of BF increases over time to reach a maximum after 40 min and thereafter tends toward a constant value indicating that no more BF are removed from the solution.

Adsorption kinetic is crucial to the process and design of the adsorption system, which determines the time required to reach equilibrium. Several kinetic models describing the diffusion of solutes on the surface and in the pores of the adsorbent have been developed. Pseudo first order, pseudo-second-order, Elovich, and intraparticle diffusion are used in this study to examine the adsorption rates of BF onto AC.

The pseudo-first-order model: The pseudo-first-order model is based on the hypothesis that the solute absorption rate with time is directly proportional to the gradient, i.e. to the difference in saturation concentration and to the quantity of solid absorbed with time [**34**]. This model is generally applicable during the initial stage of an adsorption process and the nonlinear form of the model is given by the following equation:

$$\mathbf{\log(q_e - q_t) = \log q_e - \frac{K_1}{2.303} \cdot t} \qquad \mathbf{(12)}$$

Where q_e (mg/g) and q_t (mg/g) are the amounts of the amount adsorbed at equilibrium and at time t; k_1(min^{-1}) is the rate constant in the pseudo-first-order model determined by plotting Log (q_e-q_t) versus t.

The pseudo-second-order model: This kinetic model, first proposed by Ho and McKay **[35]** is based on the assumption that the rate-limiting step is chemical sorption or chemisorption over the whole range of adsorption, involving sharing or exchange of electrons between the solute and the sorbent. This involves the adsorption of one adsorbate molecule onto two active sites on the sorbent surface; the nonlinear form of the model is given by the following equation:

$$\frac{t}{q_t} = \frac{1}{K_2 \cdot q_e^2} + \frac{1}{q_e} \cdot t \qquad (13)$$

Where k_2 (g/mg min) is the pseudo second order rate constant; q_e is determined by plotting t/q_t versus t

The Elovich model: The Elovich model is often used to interpret adsorption kinetics; it successfully describes second-order kinetics assuming an energetically heterogeneous surface **[36]** and given by the relation:

$$q_t = \frac{1}{\beta} \ln \alpha.\beta + \frac{1}{\beta} \ln t \qquad (14)$$

Where α (mg/g min) is the initial adsorption rate and β (mg/g) relates the degree of surface coverage to the activation energy involved in chemisorption.

The Intraparticle diffusion model: To identify the diffusion mechanism in the adsorption, the intraparticle mass transfer diffusion model has been proposed by Weber and Morris **[37]**:

$$q_t = K_{in}\sqrt{t} + C \qquad (15)$$

Where K_{in} is the intra-particle diffusion rate (mg/g$min^{1/2}$), q_t the amount of BF adsorbed at time t and C (mg/g) the intercept. The relationship between q_t and $t^{1/2}$ shows a multi linear curve of the experimental data on BF which reflects different types of diffusion. In order to properly interpret the experimental data, it is necessary to recognize the steps involved in the adsorption processes, which control the overall removal rate in each case.

To distinguish, whether the ongoing process follows particle diffusion or film diffusion, the kinetic data have been treated by ingenious mathematical treatment recommended by Boyd et al. **[38]** and Reichenberg **[39]**. The three consecutive steps in the adsorption of an organic/inorganic compound by a porous adsorbent are:

i) Transport of the BF to the external surface of the adsorbent (film diffusion);
ii) Transport of BF within the pores of the adsorbent except for a small amount of adsorption, which occurs on the external surface (particle diffusion);
iii) Adsorption of adsorbate on the interior surface of the adsorbent.

Consequently, the adsorption of BF on the adsorbent was directed by more than one mechanism (i.e., chemical reaction and pore-diffusion processes were involved in the uptake of BF by the tested adsorbent). If the intra-particle diffusion occurs then q_t against $t^{1/2}$ will be linear and the line will pass through the origin, indicating that intra-particle diffusion was the only rate-limiting parameter controlling the process. Otherwise, some other mechanisms are also involved. The value of the intercept gives an indication of the thickness of the boundary layer, i.e., the larger the intercept the greater is the boundary layer effect. The

value of the intercept gives an indication of the thickness of the boundary layer; the larger this value, the greater the boundary layer effect.

The constants of the different kinetic models as well as the calculation of the statistical errors obtained after modeling are grouped in Table.5. Kinetic modeling shows that the best correlation is obtained by the pseudo second order kinetic model (R^2 = 0.99) **Figures.11;** and the experimental and calculated adsorbed quantities are very close, therefore chemisorption predominates the adsorption mechanism.

Thermodynamic properties modeling studies

Effect of temperature during adsorption was utilised to get insights into the spontaneity and endothermicity/exothermicity of the adsorption process of Fuchsin Basic. The temperature is an important parameter which influences the BF adsorption on the AC surface. Its importance is not limited only to the need to understand how it affects adsorption and desorption, but also to the use of experimental results, thus allowing access to useful thermodynamic information. The variation in the adsorption capacity of BF as a function of temperature is illustrated in Figure.12. It is noted that the increase in temperature from 25 to 50 °C causes an increase in adsorption from 41 to 46 mg/g indicating a favorable adsorption for the BF. This could be due to the fact that at higher temperatures, the kinetic energy of the dye molecules is increased along with the reduction in the viscosity of the solution leading to enhanced diffusion of dye molecules into the pores of the adsorbent. The temperature has two important effects, known to increase the mobility and the diffusion rate of BF molecules through the boundary layer and into the internal pores of the adsorbent particle, due to the decrease in the viscosity of the solution.

Free energy (ΔG°), entropy (ΔS°) and enthalpy (ΔH°) were explored to provide clear insight into the spontaneity of BF adsorption on AC; Eqs. (16–19) are used to calculate adsorption thermodynamic properties:

$$\Delta G^\circ = \Delta H^\circ - T\Delta S^\circ \quad (16)$$

$$\Delta G^\circ = -RT \ln K_d \quad (17)$$

$$K_d = \frac{qe}{Ce} \quad (18)$$

$$\ln K_d = -\frac{\Delta H^\circ}{RT} + \frac{\Delta S^\circ}{R} \quad (19)$$

K_d is the distribution coefficient, q_e (mg/g) the quantity of BF adsorbed at equilibrium and C_e (mg/L) the quantity of BF in solution at equilibrium. The ratio of activity coefficients was assumed to be uniform in the dilute ranges of the solutions. As the dyes concentration in the solution approaches zero, the activity coefficient tends to unity.

The values of K_e determined from the intercept, by plotting $\ln(q_e/C_e)$ versus C_e and extrapolating to $C_e = 0$ **[40]**. The thermodynamic parameters of the BF removal were determined from adsorption data at different temperatures. The functions ΔH°, ΔS° and ΔG° obtained from the slope and intercept of the plots $\ln K_o$ versus 1/T **Figure 13 b**, are listed in **Table.7**.

Furthermore, the magnitude of the Enthalpy indicates if the process is controlled by physical adsorption (ΔH° < 20 kJ/mol) or chemical adsorption (ΔH° > 20 kJ/mol); ΔH^0 (67.421 kJ/mol). For BF obtained in this work denotes that adsorption is controlled by chemical adsorption. The standard entropy ΔS° is used to describe the randomness of an adsorption process, the positive value (0.252 kj/mol K) obtained imply an

ordered nature of the dyes adsorption. The stability and unpredictability [41] of the adsorption process are indicated by the positive values of ΔS^{o}.

Even though the drug has three degrees of freedom in the fluid phase and after adsorption, it loses one degree of freedom, therefore, the system is ordered. However, the entropy change of the entire process remains positive. As the adsorption time increases, the dye move from a nearly disordered ordered state to an ordered state within the solution, resulting in an increased rate of diffusion and removal. The negative free energy ΔG^{o} (-11.455 to - 6.415 kj/mol) at the investigated temperatures indicates a sponatenous and favorable adsorption for the BF dye.

The rate constant of the pseudo-second order kinetics at differentes temperatures obeys the Arrhenius known relation:

$$\ln K_2 = \ln A - Ea/RT \qquad (20)$$

A is a pre-exponential factor and K_2 (g/mg.min) is the pseudo-second-order kinetics constant at different temperatures. The activation energy (Ea) easily deduced by plots $\ln K_2$ vs 1/T. The plot of the linearized form (Eq.20) of the law $\ln K_2 = f(1/T)$ (**Figure.13a**) for BF enabled us to calculate the activation energies (E_a) recorded in **Table.6**. The energy E_a (48.465 kJ/mol) for BF, is characteristic of a chimisorption process, this result is in perfect correlation with the obtained results (Enthalpy is 67.421 kJ/mol).

Performance and regeneration of the adsorbent

It is instructive for a comparative purpose to give the adsorption capacity of some adsorbents available in the open literature. The values of the maximum adsorption capacity q_{max} of various adsorbent are gathered in **Table.7** We can see that the BF adsorption observed in our study is well classified compared to other researches with a maximum adsorption capacity q_{max} (34.482, 66.667 and 93.467 mg/g) at 20 , 30 and 40 °C respectively), relatively interesting with respect to other adsorbents. The differences of the dye uptakes are due to the properties of each adsorbent namely the morphology, structure, functional groups and the surface area. The AC could be an attractive adsorbent for dyes owing to the isoelectric point (pH_{pzc}). This study has given satisfactory and encouraging results, and we hope to extend to column adsorption tests under the conditions applicable to the treatment of industrial effluents.

Desorption is an inevitable process of adsorption and is an intermediate step toward regeneration. The latter is an essential tool to assess the reuse of any adsorbent for industrial applications, due to ecological concerns and sustainable development needs. For the regeneration of the adsorbent, several methods are distinguished among which we can mention regeneration: electrochemical, microbiological, thermal and chemical but we have opted for chemical regeneration because of its low economic cost.

The desorption BF of activated carbon was evaluated using three solvents NaOH, HCl, and H_2O. The desorption experiments were carried out after adsorption of BF solution of concentration 150 mg/L, pH 8, adsorbent dose 0.3 g/L and temperature of 25 °C, the activated carbon was separated from the solution by centrifugation and dehydrated at 40 °C aver night. Regeneration and reuse of adsorbents for other cycles is economically important. To validate the environmental friendliness and cost-effectiveness of AC, it is crucial to carry out the regeneration process. To carry out the desorption phase, the adsorbent is retrieved after the adsorption procedure and subjected to washing with a solution of 0.01 mol/L of NaOH, HCl, and H_2O followed by rinsing with distilled water. The results obtained reveal that all the solvents used gave very low desorption efficiencies, which confirms that the activated carbon is exhausted in the first cycle, this can be explained by the formation of new bonds due to the chemisorption process.

Possible Mechanism involved in adsorption

As previously mentioned, the intraparticule diffusion is not the only factor limiting the BF adsorption onto AC and other mechanisms can be involved simultaneously in the adsorption process of this system. In order to confirm the functional groups involved in the mechanism adsorption of BF, we compared the FTIR spectra of the activated carbon before and after the BF adsorption**.** The mechanism followed in the removal of BF on AC is shown in **Figure.14.** It includes **π-π** stacking, hydrogen bonding and electrostatic interaction. AC has a positive charge at pH< pHpzc (=7.5), on its surface promoting the attraction of the anionic dye. For pH>pHpzc, AC acquires a negative charge on its surface, thus attracting electrostatically the cationic dye BF. The hydroxyl groups present on the AC surface are involved in the hydrogen bond with the N atoms of BF and this is evident from the FTIR results: the broad hydroxyl peak in AC decreased after adsorption due to the involvement of –OH groups in the adsorption mechanism. Furthermore, adsorption is promoted by **π-π** interactions between the AC and the aromatic rings of Bf. All these mechanisms facilitate the adsorption process on the surface of the adsorbent.

Phytotoxicity study

The disposal of dye-containing water, and dye-treated water into the environment might adversely affect aquatic life and soil fertility, decreasing agricultural productivity. The phytotoxicity of these substances must therefore be evaluated in order to ensure their safety for the environment.

To highlight the influence of activated carbon and pollutants on plant germination and the environment, we conducted phytotoxycity tests. The tests were carried out in four containers, each containing 10 lentils for germination over a period of 15 days.

a) The first container contained one liter of a BF solution at a concentration of 150 ppm.
b) The second container contained tap water containing activated carbon at a concentration of 6 g/L.
c) The third container was watered only with tap water.
d) The fourth container contains a mixture of tap water with Fuchsin and activated carbon.
After 15 days of germination **(Figure.15)**, we observe that:

The number of lentil seeds that germinated in the first container is 9 out of 10 seeds, which is 90%.
The same rate of germination is observed for the third container with tap water, also at 90%.
For the container containing activated carbon, only a rate of 70% is obtained.
The fourth container, containing the mixture of activated charcoal and Fuchsin, has the lowest germination rate of 40%.

In conclusion, the best germination is obtained in the presence of BF yield (90%) compared to water (R = 90%). This can be explained by the fact that BF is probably part of the composition of fertilizers; therefore BF is not harmful to plants. On the other hand, activated carbon (R = 40%) shows a great lightness towards plants and watercourses and consequently on aquatic, animal and human life.

4. Conclusion

Globally, there is a need for a sustainable approach and the development of efficient processes for water treatment. Dye removal by new generation adsorbents has been shown to be highly effective. In this study, the statistical methodology, Response Surface Design, was found to be effective and reliable in optimizing the adsorption conditions, which showed significant effects on the removal of BF.

Response surface plots were used to estimate the interactive effects of four independent variables (initial dye concentration, pH, and adsorbent dose) on the adsorption percentage. The second-order mathematical model was developed by regression analysis of experimental data obtained from 15 batch tests.

The optimal conditions obtained by the exploitation of 3D contours and surfaces are: (initial concentration of BF: 178.074 mg/L, pH of the initial solution: 6.78 and the dose of CA: 0.3837 g at temperature: 25 °C)

Different isotherm models were used to fit the experimental data, the results indicate that the Langmuir model offers the best correlation; the maximum adsorption capacities obtained are respectively 34.482, 66.667 and 93.467 mg/g at temperatures 20, 30 and 40 °C

A confirmation test was undertaken to determine the accuracy and reliability of the optimization with maximum removals of BF (96.149%). Error analyses were used to measure the goodness of fit. Kinetic modeling showed that adsorption obeys the pseudo-second-order kinetic model (R^2 = 0.999)

The effect of temperature on adsorption isotherms allowed obtaining the following thermodynamic functions: The negative values of free energy ΔG^o (-11.455 to - 6.415 kJ/mol) and a positive enthalpy ΔH^o (67.421 kJ/mol), confirming the spontaneous and endothermic nature of BF adsorption on CA. The positive entropy ΔS^o (252 J/mol.K) shows an accumulated random character of the solid-liquid interface during adsorption. The adsorption of the FB dye onto the AC surface can be explained by several possible interactions including π-π stacking, electrostatic forces, pores filling, and hydrogen bonding. The photochemical study reveals that CA is harmful to germination and soil and that BF positively influences plant germination.

Ethics Approval
Not applicable

Consent for Publication
All authors provided their consent for publication.

Conflict of Interest
The authors declare no competing and conflict of interests.

Data Availability

Not applicable

Code Availability

Not Applicable

Funding
Not Applicable

Consent to Participate
All authors provided their consent for publication.

Authors Contributions

M. ABBAS: Conceptualization, Methodology, Visualization,
M. ABBAS, S Chennouf: Investigation, Validation, Data curation, Writing – original draft,
M. TRARI, Z Harrache review & editing.

References

[1] Patel H., Routoula E., Patwardhan S. V. Decontamination of anthraquinone dyes polluted water using bioinspired silica as a sustainable sorbent. Silicon, 2022, Vol.14, 1235 -1245

[2] Adeyemo A. A., Adeoye I. O., Bello O. S. Adsorption of dyes using different types of clay: a review Applied Water Science 2017, Vol. 7, 543-568

[3] Yaseen D. A., Scholz M. Textile dye wastewater characteristics and constituents of synthetic effluents: a critical review. International journal of Environmental Science and Technology 2019, vol. 16, 1193-1226

[4]. de Lima R. O. A., Bazo A. P., Salvadori D. M. F., Rech C. M., de Palma Oliveira D., de Aragão Umbuzeiro G. Mutagenic and carcinogenic potential of a textile azo dye processing plant effluent that impacts a drinking water source. Mutation Research/Genetic Toxicology and Environmental Mutagenesis, 2007, vol. 626, Issue 1-2, 53-60

[5] RD Lillie, HJ Conn - Biological Stains - A handbook on the nature and uses of the dyes employed in the biological laboratory. Eighth ed., Williams & Wilkins 1969

[6] L. Luna, Manual of histologic staining methods of the Armed Forces Institute of Pathology third ed., McGraw–Hill, New York, 1968, 222.

[7] F.L. Carson, Histotechnology : A Self-Instructional Text, second ed., American Society Clinical Pathology, 1997. Chicago: ACSP Press

[8] J. Crookham, J.R. Dapson, Hazardous Chemicals in the Histopathology Laboratory, second ed., Anatech, 1991.

[9] A.A. Fisher, Irritant and toxic reactions to phenol in topical medications. Cutis 1980, 26 363-390.

[10] Sarah C. F. Rogers, Desmond Burrows, Desmond Neill, Percutaneous absorption of phenol and methyl alcohol in Magenta Paint B.P.C. British Journal of Dermatology, 1978, Vol. 98, Issue 5, 559–560

[11] Neil A. Littlefield, Boon-Nam Blackwell, Cynthia C. Hewith, David W. Gaylor, Chronic Toxicity and Carcinogenicity Studies of Gentian Violet in Mice Fundamental and Applied Toxicology, 1985, Vol.5, Issue 5, 902–912

[12] K.A. Matis, A.I. Zouboulis, D. Zamboulis, A.V. Valtadoron, Sorption of As(V) by Goethite Particles and study of their Flocculation. Water Air Soil Pollut. 1999, Vol.111, 297-316

[13] O. Duman, S. Tunç, T.G. Polat Adsorptive removal of triarylmethane dye (Basic Red 9) from aqueous solution by sepiolite as effective and low-cost adsorbent Microporous Mesoporous Mater., 2015, Vol.210, 176-184

[14] Sahmoune Mohamed Nasser, Moussa Abbas and Mohamed Trari, Understanding the rate-limiting step adsorption kinetics onto biomaterials for mechanism adsorption control. Progress in Reaction Kinetics and Mechanism 2024, Vol.49, 1–26

[15] El Gaidoumi A., Arrahli A., Loqman A., Baragh F., El Bali B., Kherbeche A. Efficient sol-gel nanocomposite TiO_2-clay in photodegradation of phenol: comparison to Labe-made and commercial photocatalysts Silicon , 2022 ,14 4672622 10, 5401 -5414

[16] Moussa Abbas & Mohamed Trari. Mass transfer process in the adsorption of Cibacron Blue (CB) on untreated peapods (UPPs): kinetic and thermodynamic studies. Water Practice & Technology 2024, Vol. 19 No 11, 4454

[17]. Moussa Abbas Depollution of water contaminated by Yellow Bezacryl (YB) using TiO2 nano photocatalyst: kinetic study, isotherms modeling and adsorption mechanism. Nanotechnology for Environmental Engineering 2025; Vol.10, 5

[18] Tounsia AKSIL, Moussa ABBAS and Mohamed TRARI, Elaboration of a new Activated Carbon derived from the Crown of Oak (ACOW) to removal the toxic Iodine: Kinetic, Isotherms modelling and Thermodynamics Study. Chemistry and Ecology, 2024, Vol. 40, Issue 9, 1001-1027

[19] Daouda, M. M. A., Akowanou, A. V. O., Mahunon, S. E. R., Adjinda, C. K., Aina, M. P. & Drogui, P., Optimal removal of diclofenac and amoxicillin by activated carbon prepared from coconut shell through response surface methodology. South African Journal of Chemical Engineering, 2021, 38(1), 78-89.

[20] Moussa Abbas & Mohamed Trari, Removal of Amoxicillin From Wastewater Onto Activated Carbon: Optimization of Analytical Parameters by Response Surface Methodology. Dose-Response: An International Journal 2024, 1–15

[21] Moussa Abbas, Tounsia Aksil & Mohamed Trari, Removal of methylene blue dye from water by an activated carbon: optimisation of analytical parameters by response surface methodology. Chemistry and Ecology, 2025, Vol.41, Issue 9, 1205-1231

[22] Samiya Merrad, Moussa Abbas, Mohamed Trari, Adsorption of Malachite Green onto Walnut Shells: Kinetics, Thermodynamic, and Regeneration of the Adsorbent by Chemical Process. Fibers and Polymers 2023, Vol.24, 1067–1081

[23] Fu JF, Zhao YQ, Xue XD, Li WC, Babatunde AO. Multivariate-parameter optimization of acid blue-7 wastewater treatment by Ti/TiO2 photoelectrocatalysis via the Box-Behnken design. Desalination 2009; Vol.243, 42–51.

[24] Moussa Abbas and Mohamed Trari, Engineering of Natural Clay-Based Materials to Eliminate Toxic Pb(II): Kinetic, Thermodynamic, and Adsorption Mechanism Study. Protection of Metals and Physical Chemistry of Surfaces, 2025, Vol. 61, N°. 3, 530–540.

[25] Virkutyte J, Rokhina E, Jegatheesan V. Optimisation of Electro-Fenton denitrification of a model wastewater using a response surface methodology. Bioresour Technol. 2010; Vol.101(5), 1440-1446

[26]. Masoud Z, Wan Mo AWD, Mohamed KA. Optimization of the activity of CaO/Al_2O_3 catalyst for biodiesel production using response surface methodology. Appl Catal, A. 2009, Vol.366(1), 154-159.

[27] Harrington EC The desirability function. Industrial Quality Control 1965, Vol.21, 494–498.

[28] Derringer G and Suich R Simultaneous optimization of several response variables. Journal of Quality Technology 1980, Vol.12(4), 214–219.

[29] Langmuir I. The adsorption of gases on plane surface on glass, mica and platinum. J Am Chem Soc. 1918; Vol.40(9), 1361-1403.

[30] Freundlich H. Concerning adsorption in solutions. Z Phys Chem Stoch. 1906; Vol.57, 385-470.

[31] Temkin M, Pyzhev V, Kinetics of ammonia synthesis on promoted iron catalysts. Acta Physicochim. URSS 1940, Vol.12, 327-356.

[32] Hasan P, Hamid RG, Amir HM, Mina P, Ali A. Activated carbon derived fromdate stone as natural adsorbent for phenol removal from aqueous solution. Desalination Water Treat. 2017; Vol.72, 406-417.

[33] Zahia Harrache , Moussa Abbas Elimination of a Cationic dye in Aqueous Solution by Adsorption on Activated Carbon: Optimization of Analytical Parameters, Modeling and Thermodynamic Study. .Journal of Engineered Fibers and Fabrics 2022, Vol.17, 1-12

[34] Lagergren S. Kung. About the theory of so-called adsorption of soluble substances. Sven Vetenskapsakad Handingarl. 1898; Vol.24, 1-39.

[35]. Ho YS, McKay G. Kinetic models for the sorption of dye from solution by wood. J Environ Sci Health B. 1998; Vol.76(4): 183-191.

[36] Cheung CW, Porter JF, Mckay G. Sorption kinetic analysis for the removal of cadmium ions from effluents using bone char. Water Res 2001; Vol.35, 605–612.

[37] Weber MJ and Morris J Kinetic of adsorption on carbon from solution. Journal of the Sanitary Engineering Division, American Society of Civil Engineers (1963), Vol.89 (2): 31–60.

[38] G. E. Boyd, A. W. Adamson and L. S. Meyers, "The Exchange Adsorption of Ions from Aqueous Solutions by Organic Zeolites. II. Kinetics," Journal of the American Chemical Society, 1947, Vol.69, No. 11, 2836-2848.

[39] D. Reichenberg, Properties of Ion-Exchange Resins in Relation to their Structure. III. Kinetics of Exchange J. Am. Chem. Soc. 1953, Vol.75, Issue 3, 589.

[40] Qian Li , Qin-Yan Yue , Yuan Su, Bao-Yu Gao, Hong-Jian Sun . Equilibrium, thermodynamics and process design to minimize adsorbent amount for the adsorption of acid dyes onto catoinic polymer- loaded bentonite. Chemical Engineering Journal 2010, Vol.158(3), 489–497.

[41] Yao, X., Ji, L., Guo, J., Ge, S., Lu,W., Cai, L., Wang, Y., Song,W. & Zhang, H. Magnetic activated biochar nanocomposites derived from wakame and its application in methylene blue adsorption. Bioresource Technology 2020**,** Vol.302, 122842.

[42] M. Abbas, Removal of Basic Fuchsine (BF) in aqueous solution by Adsorption Process onto 'Prunus Cerasefera' (LPC) - Kinetics, Isotherm modeling and Thermodynamic Study, 2022,

[43] V. K. Gupta, A. Mittal, V. Gajbe, et J. Mittal, « Adsorption of basic fuchsin using waste materials—bottom ash and deoiled soya—as adsorbents », J*ournal of Colloid and Interface Science*, vol. 319, n° 1, p. 30-39, mars 2008,

[44] M. El Haddad, « Removal of Basic Fuchsin dye from water using mussel shell biomass waste as an adsorbent: Equilibrium, kinetics, and thermodynamics », *Journal of Taibah University for Science*, 2016, Vol. 10, n° 5, p. 664-674,.

[45] M. El-Azazy, A. S. El-Shafie, A. Ashraf, et A. A. Issa, Eco-structured biosorptive removal of basic fuchsin using pistachio nutshells: a definitive screening design—based approach , *Applied Sciences*, vol. 9, n° 22, 4855, 2019.

[46] S. Kalita, M. Pathak, G. Devi, H. P. Sarma, K. G. Bhattacharyya, A. Sarma and A. Devi Utilization of Euryale ferox Salisbury seed shell for removal of basic fuchsin dye from water: equilibrium and kinetics investigation », *RSC Adv.*, 2017, Vol. 7, n° 44, 27248-27259

[47] Y.-H. Zhao, J.-T. Geng, J.-C. Cai, Y.-F. Cai, et C.-Y. Cao, Adsorption performance of basic fuchsin on alkali-activated diatomite , Adsorption Science & Technology, 2020, Vol. 38, n° 5-6, 151-167

[48] W. Bessashia, Y. Berredjem, Z. Hattab, et M. Bououdina, Removal of Basic Fuchsin from water by using mussel powdered eggshell membrane as novel bioadsorbent: Equilibrium, kinetics, and thermodynamic studies, Environmental Research, 2020, Vol.186, 109484

[49] A. Kumar, U. Dixit, K. Singh, S. Prakash Gupta, et M. S. Jamal Beg, Structure and Properties of Dyes and Pigments , in *Dyes and Pigments - Novel Applications and Waste Treatment*, R. Papadakis, Éd., IntechOpen, 2021.

[50] A. Ali Ahmed, Z. Hattab, Y. Berredjem, S. Hamoudi, et R. Djellabi, Valorization of Silybum marianum seed shells waste as biosorbent for basic fuchsin dye removal from water: kinetics, isotherms, and thermodynamic studies , *Desalination and Water Treatment*, 2024,Vol. 317, 100278,

[51] Jordana Georgin , Dison Franco[b], Fernanda Caroline Drumm , Patrícia Grassi, Matias Schadeck Netto , Daniel Allasia , Guilherme Luiz Dotto Powdered biosorbent from the mandacaru cactus (cereus jamacaru) for discontinuous and continuous removal of Basic Fuchsin from aqueous solutions , *Powder Technology*, 2020, Vol. 364, 584-592

[52] Aïssatou Alioune Gaye, Nicolas Cyrille Ayessou, Bio-sorption of Methylene Blue and basic fuchsin from aqueous solution onto defatted Carica papaya seeds mechanism and effect of operating parameters on the adsorption yield. IOSR Journal of Environmental Science, Toxicology and Food Technology 2020, Vol. 14, Issue 2, 24-33

[53] X. Li, L. Xie, X. Yang, et X. Nie, Adsorption behavior and mechanism of β-cyclodextrin–styrene-based polymer for cationic dyes , RSC Adv., 2018, Vol.8, N° 70, 40321-40329

[54] E. P. Fernandes, Társila S. Silva , CeniraM. Carvalho , Rangabhashiyam Selvasembian , Nhamo Chaukura[e], Leonardo M.T.M. Oliveira , Simoni M. Plentz Meneghetti, Lucas Meili Efficient adsorption of dyes by γ-alumina

synthesized from aluminum wastes: Kinetics, isotherms, thermodynamics and toxicity assessment , Journal of Environmental Chemical *Engineering*, 2021,Vvol. 9, N° 5, 106198

[55] H Pu, P Tang, L Zhao, Q Sun, Y Zhai, Z Li, N Gan, Y Liu, X Ren, H Li Preparation of a carboxymethyl β-cyclodextrin polymer and its rapid adsorption performance for basic fuchsin , *RSC Adv.*, 2020, Vol. 10, N° 35, 20905-20914

[56] Y. Guan, S. Wang, X. Wang, C. Sun, Y. Wang, et L. Hu, Preparation of mesoporous Al-MCM-41 from natural palygorskite and its adsorption performance for hazardous aniline dye-basic fuchsin , Microporous and Mesoporous Materials, 2018, Vol. 265, 266-274

Table.1: Independent Variables and Their Levels Used for Box- Behnken Design.

Parameters	cooded Variables			Parameters	Reels Variables		
X1	-1	0	+1	Dose (g)	0.1	0.3	0.5
X2	-1	0	+1	pH	6	8	10
X3	-1	0	+1	Con. (mg/L)	100	150	200

Table.2: Box-Behnken Experimental Design Matrix and Responses (R_{exp} (%) and R_{pred} (%) for Elimination of BF Onto AC.

Run	Dose	ph	C	R_{exp} (%)	R_{pred} (%)	Residual
1	0.3	10	100	82.67	85.03	- 2.360
2	0.3	10	200	87.73	88.03	- 0.303
3	0.3	8	150	88.47	87.45	1.020
4	0.1	8	100	94.98	92.62	2.360
5	0.5	8	100	82.67	83.30	- 0.630
6	0.1	8	200	87.01	88.36	- 1.350
7	0.3	6	100	92.16	90.18	1.980
8	0.3	8	150	98.37	100.00	- 1.980
9	0.3	6	200	97.39	96.76	0.630
10	0.1	10	150	87.73	88.03	- 0.303
11	0.5	10	150	88.64	88.03	0.607
12	0.5	6	150	87.03	86.64	0.386
13	0.5	8	200	97.32	98.34	- 1.020
14	0.3	8	150	82.96	83.35	- 0.386
15	0.1	6	150	92.28	90.93	1.350

Table. 3: Analysis of Variance (ANOVA) for Response Surface Quadratic Model.

Source	*Sum of Squares*	*df*	*Coded. coef.*	*Rels. Coef.*	*Mean Square*	***F-value***	***p-value***
Model	375.44	9	88.03	+120.10073	41.72	7.93	0.0173
Linear Parameters							
X1- (Dose)	17.26	1	1.47	+70.41250	17.26	3.28	0.1299
X2- (pH)	221.45	1	5.26	-12.35208	221.45	42.09	**0.0013**
X3- (Conc.)	0.2592	1	0.1800	-0.068200	0.2592	0.0493	0.8331
interaction Parameters							

X1X2	1.45	1	0.6025	+1.50625	1.45	0.2760	0.6218
X1X3	21.62	1	-2.33	-0.232500	21.62	4.11	0.0985
X2X3	5.62	1	-1.19	-0.011850	5.62	1.07	0.3489
Quadratic parameters							
X_1^2	26.58	1	-2.68	-67.07292	26.58	5.05	**0.0745**
X_2^2	61.38	1	4.08	+1.01927	61.38	11.66	**0.0189**
X_3^2	14.32	1	1.97	+0.000788	14.32	2.72	0.1599
Residual	26.31	5			5.26		
Lack of Fit	25.76	3			8.59	31.10	**0.0313**
Pure Error	0.5521	2			0.2760		
Cor Total	401.75	14		**Std. Dev.**	2.29	**R^2**	0.9345
				C.V. (%)	2.55	**Adj. R^2**	0.8166

Table.4: Different Parameters for Adsorption Isotherm Models for the Removal of BF onto AC at different temperatures.

Langmuir	Freundlich	Temkin	Elovich	
T= 20 ^0C	Q_{max} (mg/g) = 34.482	1/n =0.462	α = 0.753	Q_{max} (mg/g) =19.763
	K_L (L/g) =0.105	n = 2.16	β =8.288	K_E = 0.1285
	R_L (0.045-0.087)	K_F (mg/g) = 4.18	ΔE (kJ/mol) =10.12	
	0.999	0.908	0.80	0.838
	2.62 $.10^{-4}$	0.422	330.17	2222.15
R^2				
RSS				
T= 30 ^0C	Q_{max} (mg/g) = 66.667	1/n =0.4712	α (L/mg) = 0.924	Q_{max} (mg/g) = 31.25
	K_L (L/mg) =0.1145	n = 2.12	β = 16.416	K_E (L/mg) = 0.0265
	R_L (0.042-0.080)	K_F (mg/g) = 10.39	ΔE (kJ/mol) =10.23	
	0.992	0.966	0.991	0.990
	1.83 10^{-5}	0.0537	17.853	0.0189
R^2				

RSS				
T= 40 ^{0}C	Q_{max} (mg/g) = 93.467	1/n = 0.596	α = 0.372	Q_{max} (mg/g) = 51.28
	K_L (L/mg) = 0.0353	n = 1.67	β = 20.23	K_E (L/mg) = 0.0705
	R_L (0.124-0.221)	K_F (mg/g) = 5.52	ΔE (kJ/mol) =12.03	0.954
		0.991	0.959	0.0382
	0.998	0.0168	86.337	
	4.21 10^{-6}		.	
R^2				
RSS				

Table.5: Different Parameters for Adsorption Kinetics Models for the Removal of BF onto AC.

	Second	Order				First	Order		
C_o (mg/L)	Q_{ex} (mg/g)	Q_{cal} (mg/g)	R^2	ΔQ/Q (%)	K_2 (g/mg.mn)	Q_{cal} (mg/g)	R^2	ΔQ/Q (%)	K_1 (mn^{-1})
100	48.72	50.761	0.999	0.0402	0.01848	31.55	0.93	60	0.274
150	74.70	77.700	0.997	0.0386	0.01589	0	0.913	0.07	0.338
200	96.80	100.00	0.999	0.032	0.01466	43.45	0.872	1.30	0.268
						1			
						41.97			
						6			

		Elovich			Diffusion		
C_o (mg/L	R^2	β (g/mg)	α (mg/g.mn)	C_o (mg/L)	K_{in} $mg/gmn^{1/2}$	R^2	C (mg/g)
100	0.775	0.13386	273.394	100	16.735	0.969	1.673
150	0.706	0.0928	5015.6		0.6342	0.558	45.16
200	0.679	0.0899	558.948	150	26.741	0.968	2.313
					0.1815	0.924	73.72
				200	34.393	0.926	6.489
					0.5552	0.888	93.84

Table.6: Thermodynamic functions ΔG°, ΔH° and ΔS° of BF adsorbed onto AC

T (K)	1/T (K^{-1})	LnK_2	LnKe	ΔG° (KJ/mol)	ΔH° (KJ/mol)	ΔS° (kJ/mol.K)	Ea (KJ/mol)

293	0.003413	- 4.023	2.639	- 6.415			
303	0.003300	-3.342	2.965	- 8.935			
308	0.003247	-3.00	4.046	- 10.195	67.421	0.252	48.465
313	0.003195	-2.75	4.399	- 11.455			

Table.7: Comparison of maximum adsorption capacity of BF with other adsorbents. reported in the Literature.

Adsorbent	teq (min)	C (mg/L)	Q_{max} (mg/g)	pH	Ref
Prunus Cerasefera' (LPC)	50	100-200	158.73	7-10	[42]
Deoiled soya	60	80	13	9	[43]
CalcinedMussel Shell (CMS)	240	60	141.65	9	[44]
RawPistachioNutshells (RPNS)	30	30	118.2	9	[45]
Euryale ferox Salisbury seed shell (E.ferox)	120	40	19.48	6	[46]
Alkali-activated diatomite	30	15	4.85	6	[47]
Eggshell membrane	60	250	48	6	[48]
$Ni_3 Si_2 O_5 (OH)_4$	180	50	120.7	7	[49]
Silybummarianum seed shells (SMSS)	60	10	7.142	12	[50]
Mandacaru (Cereusjamacaru) leaves (PML)	150	100	398.90	8	[51]
Garicapapayaseeds(CPS)	180	50	6.01	11	[52]
β-cyclodextrin-styrene-based polymer	90	50	29.6	6	[53]
γ-alumina	120	50	32.92	9	[54]
β-cyclodextrin-carboxymethyl cellulose-grapheneoxide composite	150	100	6.5	6	[55]
Al-MCM-41	240	60	54	5	[56]
Activated carbon	20 20 20	100-200 100-200 100-200	34.482, T = 20 °C 66.667, T = 30 °C 93.467, T = 40°C	8	This study

Figure.1: Effect of pH on the adsorption capacity of BF onto A

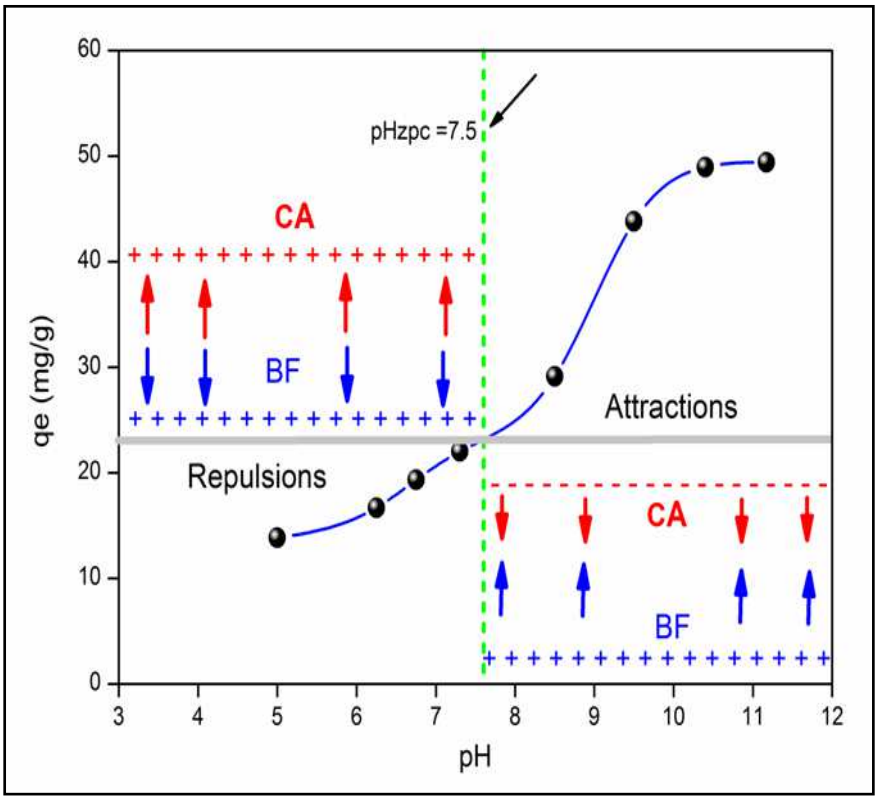


Figure.2: Isotherms sorption and desorption of N_2 for specific surface determination

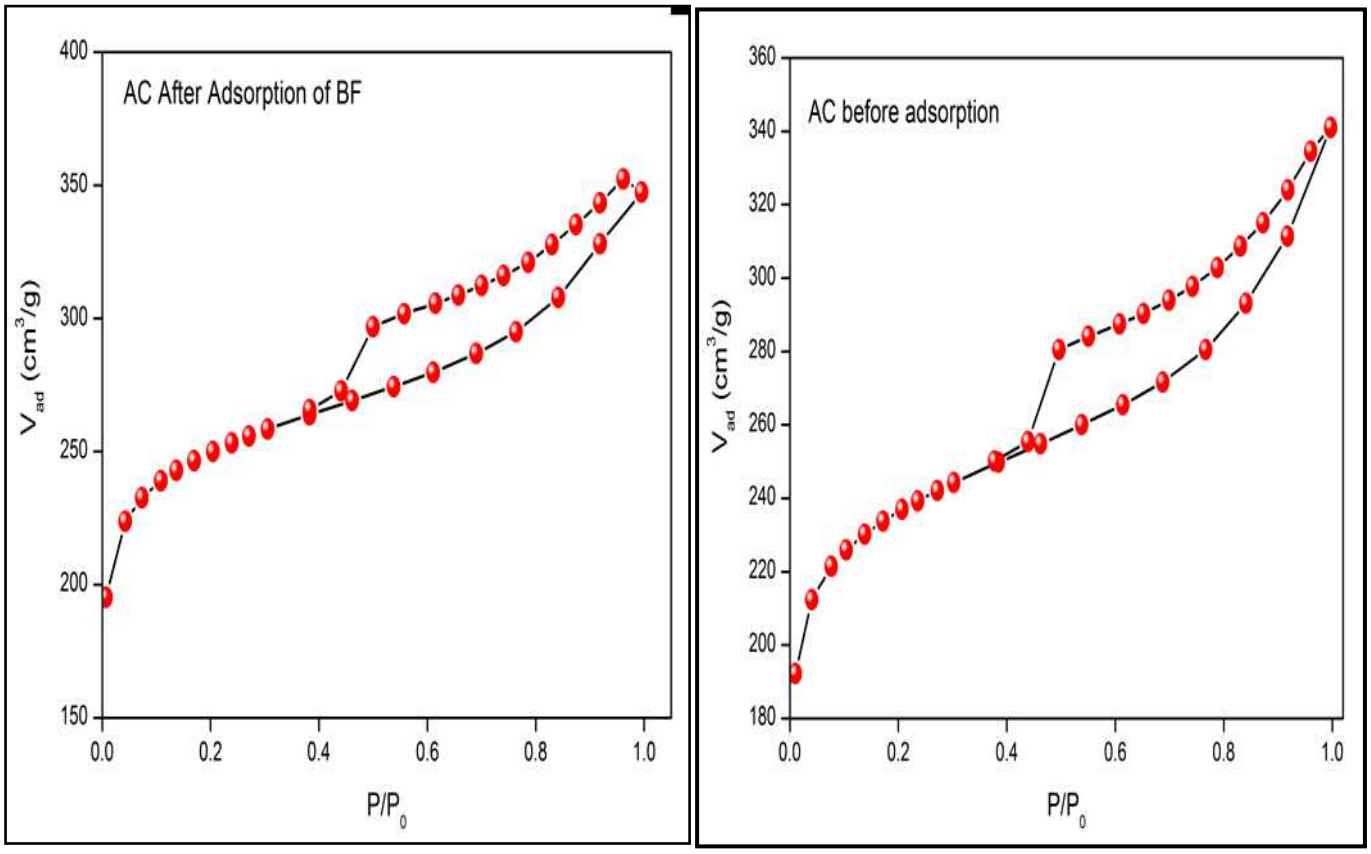


Figure.3: SEM images of activated carbon before and after adsorption of BF.

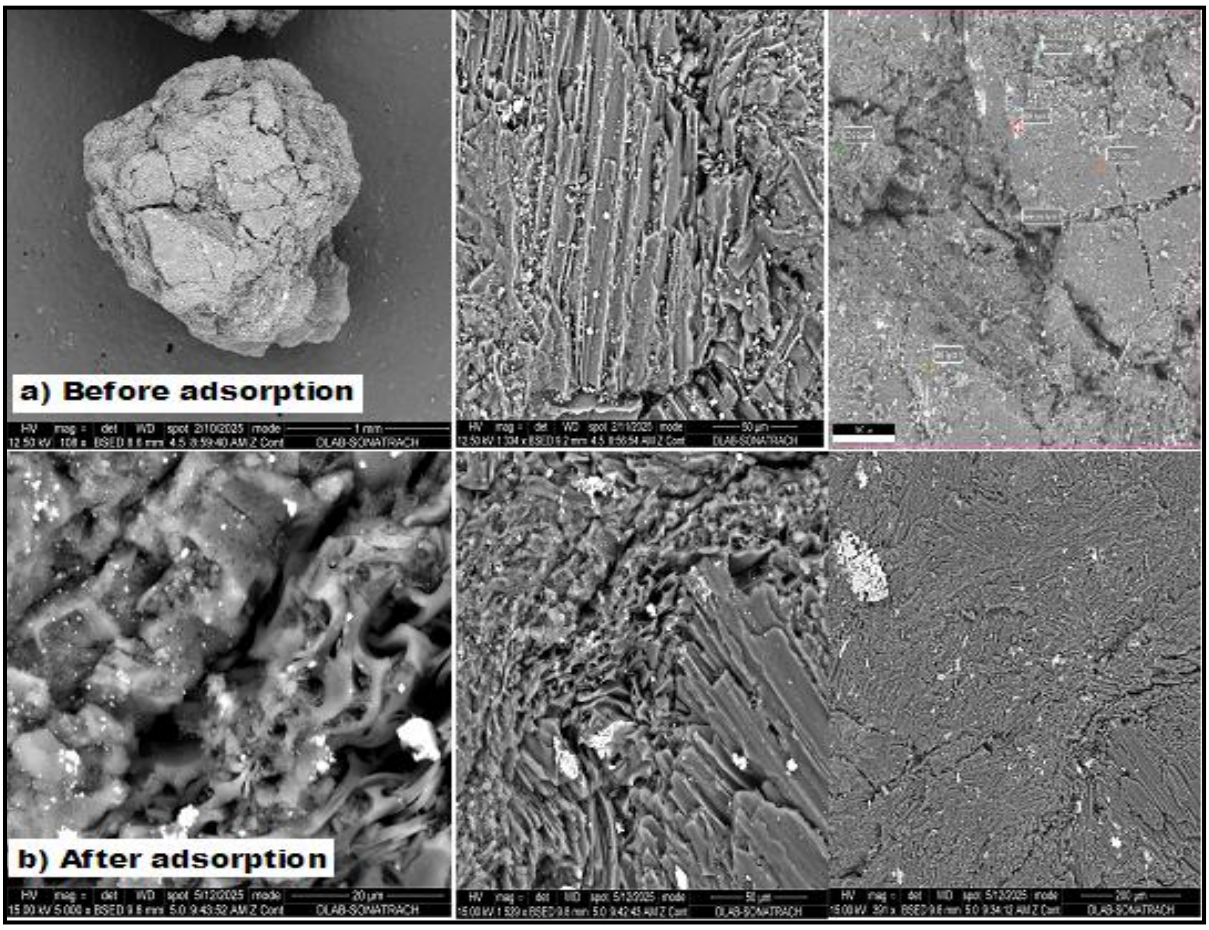


Figure.4: FTIR spectrum of activated carbon before and after adsorption of BF.

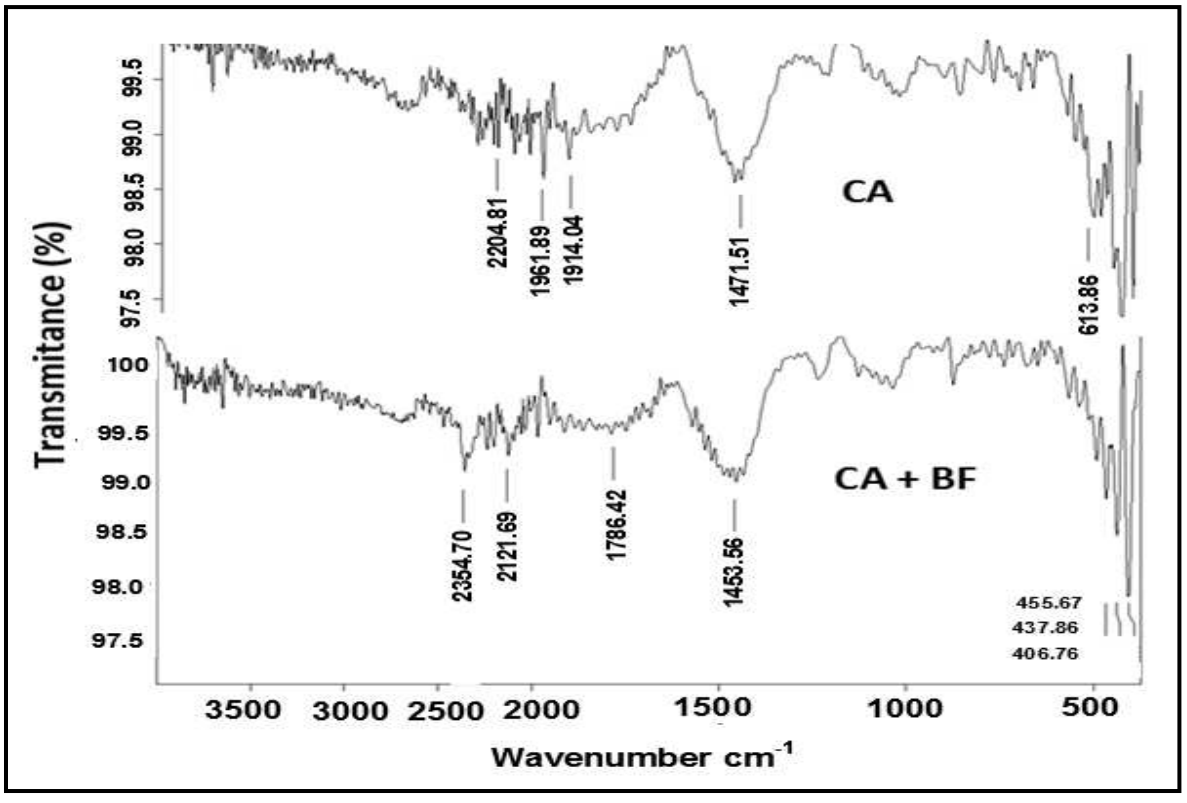


Figure.5: Histogram of adsorption amount comparison and Plot of Actual values vs . predicted values for MB adsorption onto AC.

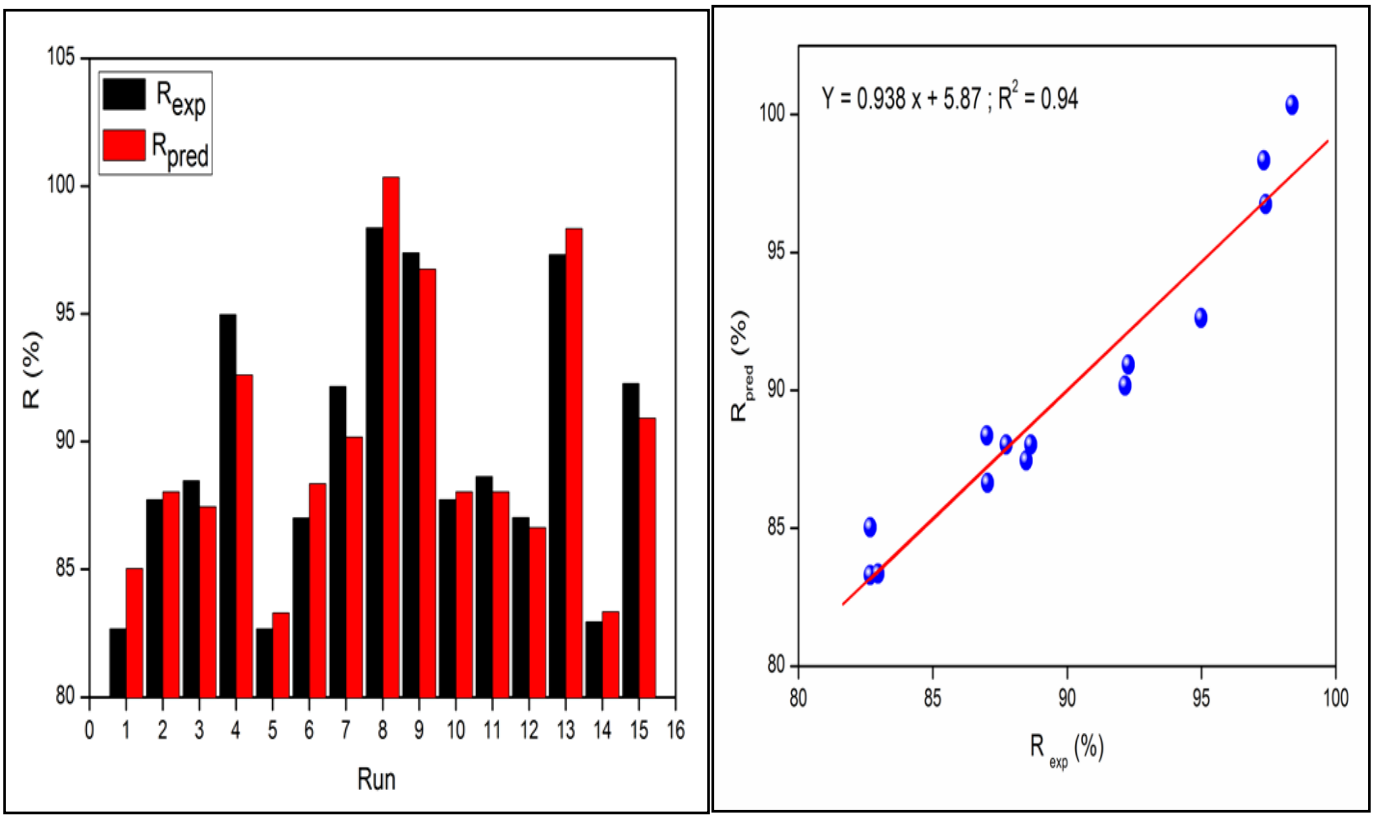


Figure.6: Response surface plots and contour plots for BF adsorption onto AC **a)** Solution pH-Adsorbent dosage, **b)** Adsorbent dosage-Concentration and **c)** Solution pH-Concentration.

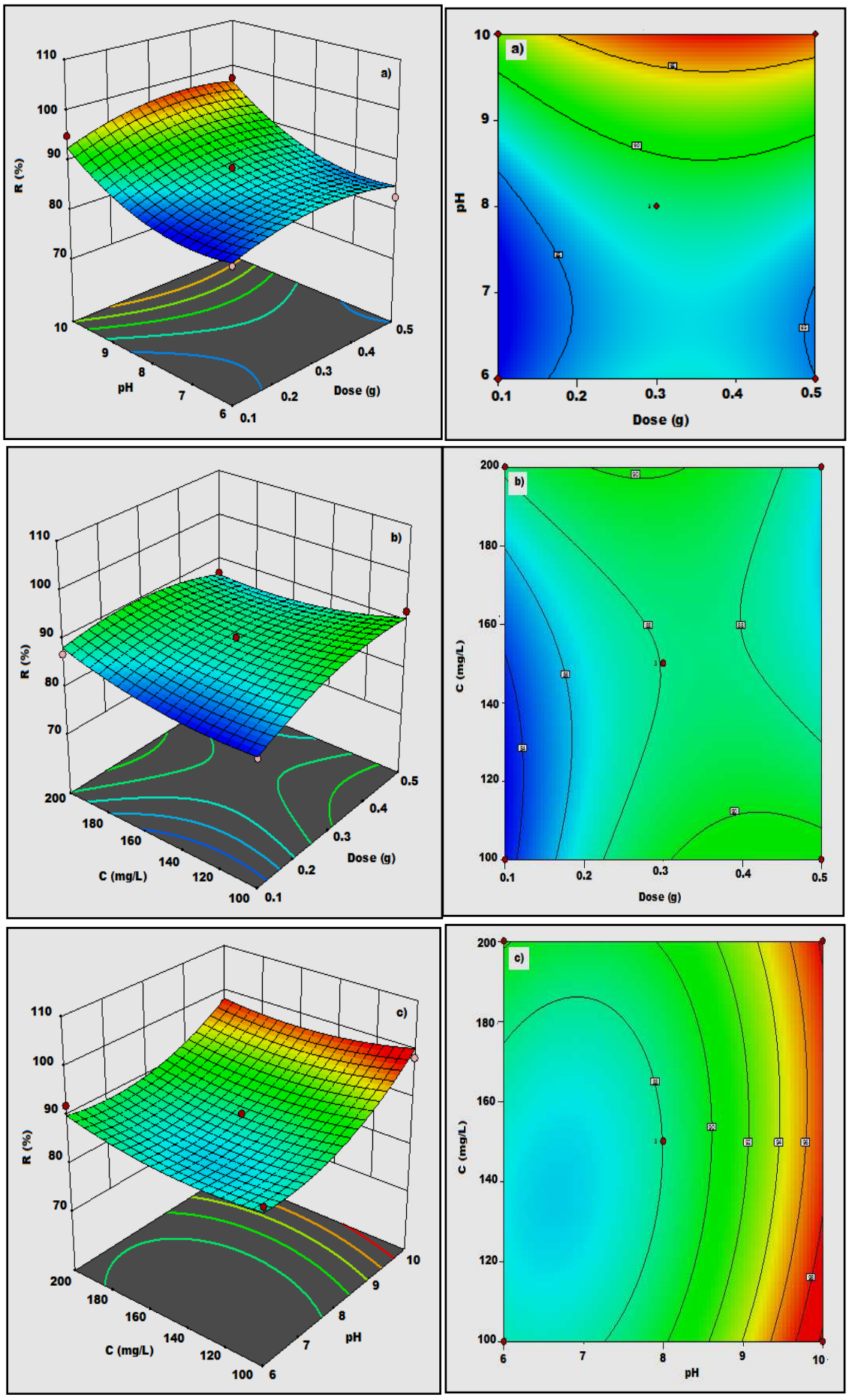


Figure.7: Optimisation of analytical parameters by the desirability function

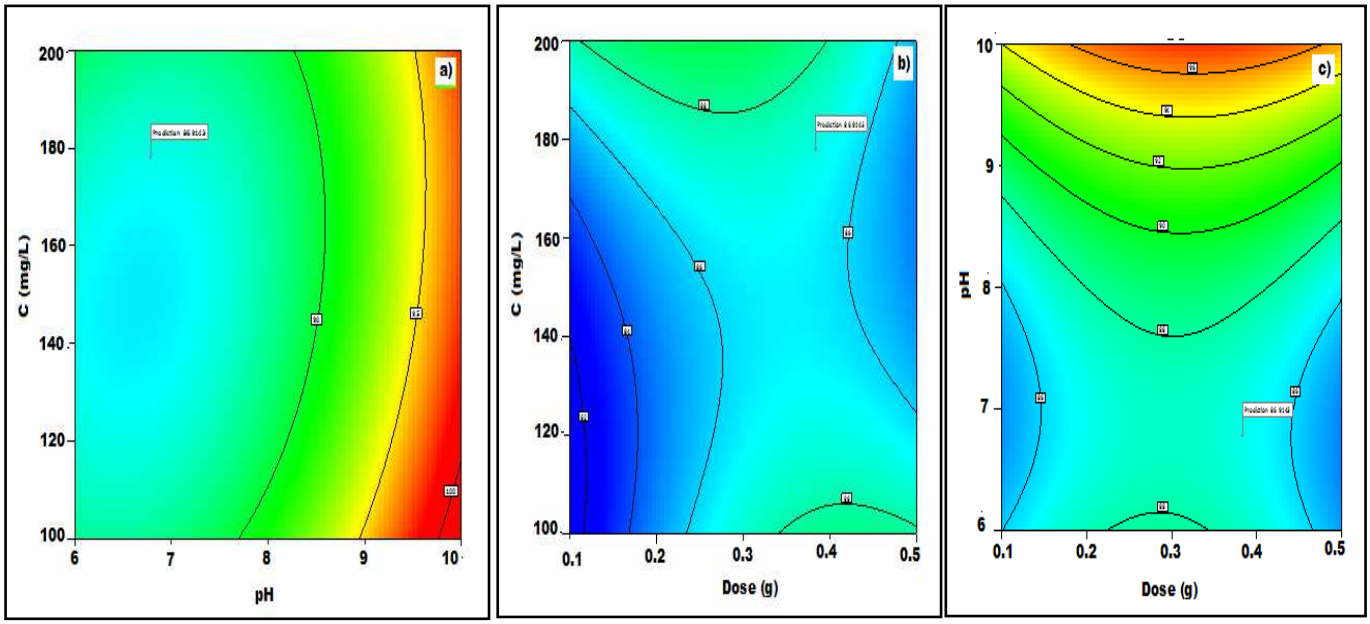


Figure.8: Diagram of the interaction effects of pH, concentration and dose factors.

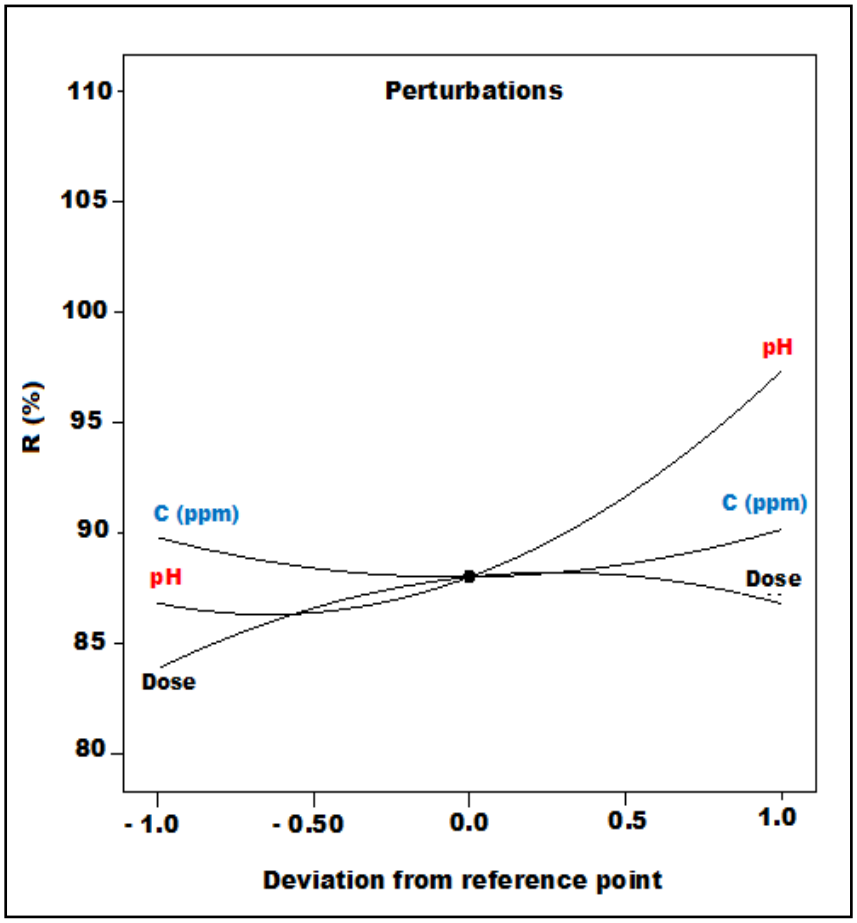


Figure.9: Isotherms modeling at different Temperatures

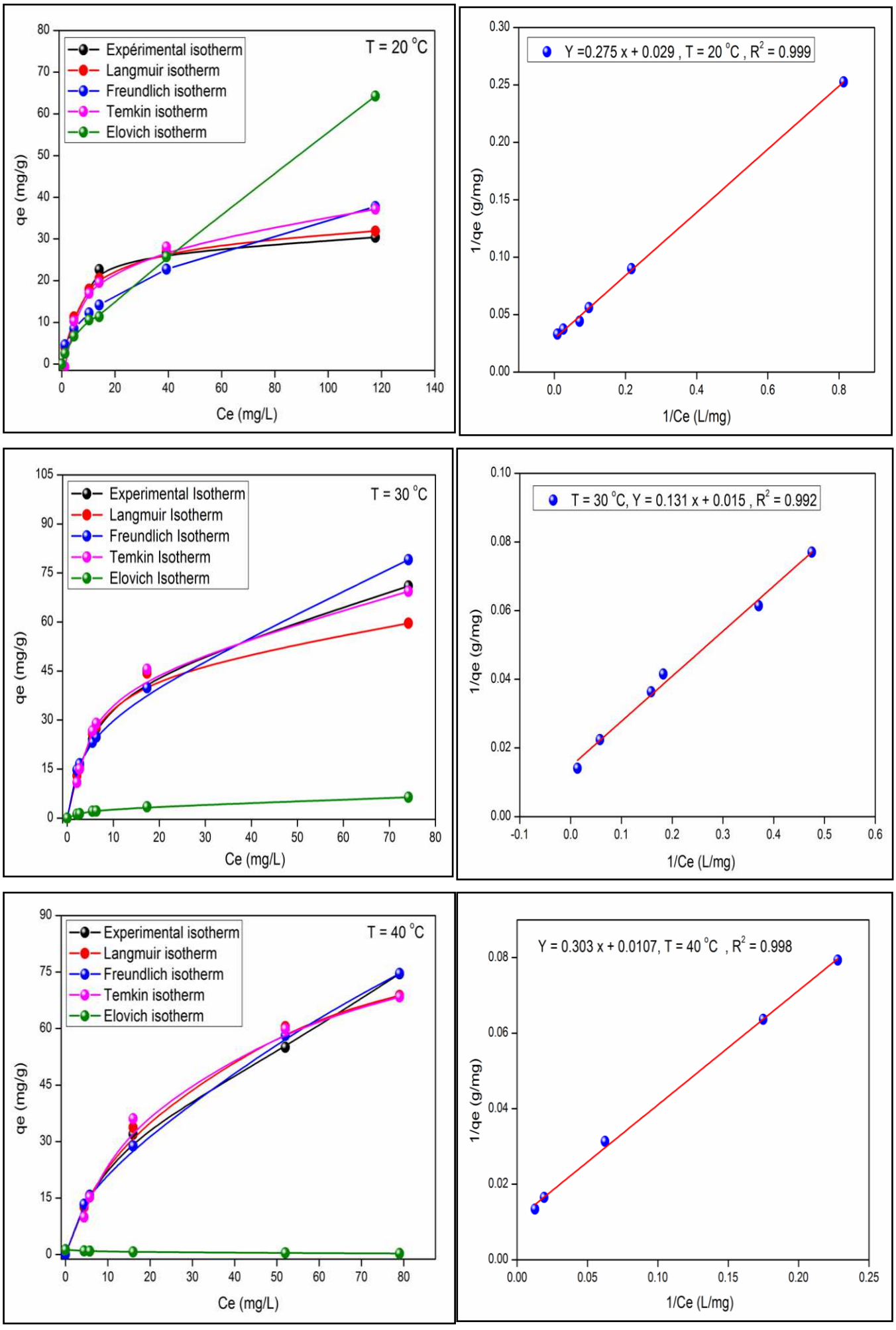


Figure.10: Effect of Concentration and contact time of the adsorption of BF onto AC

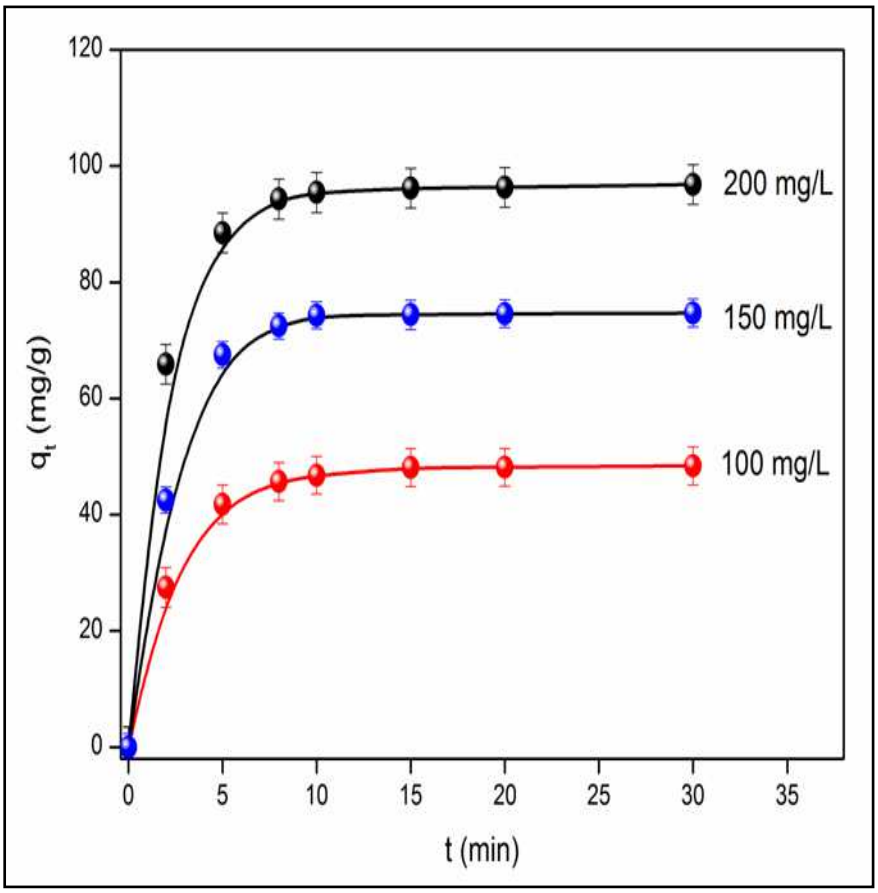
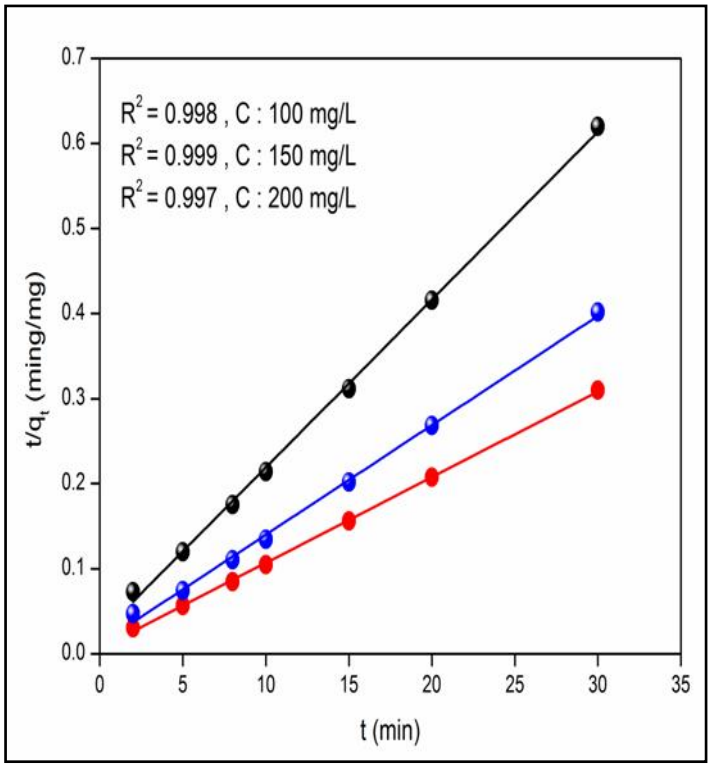


Figure.11: Modeling Kinetics by pseudo-first and second order



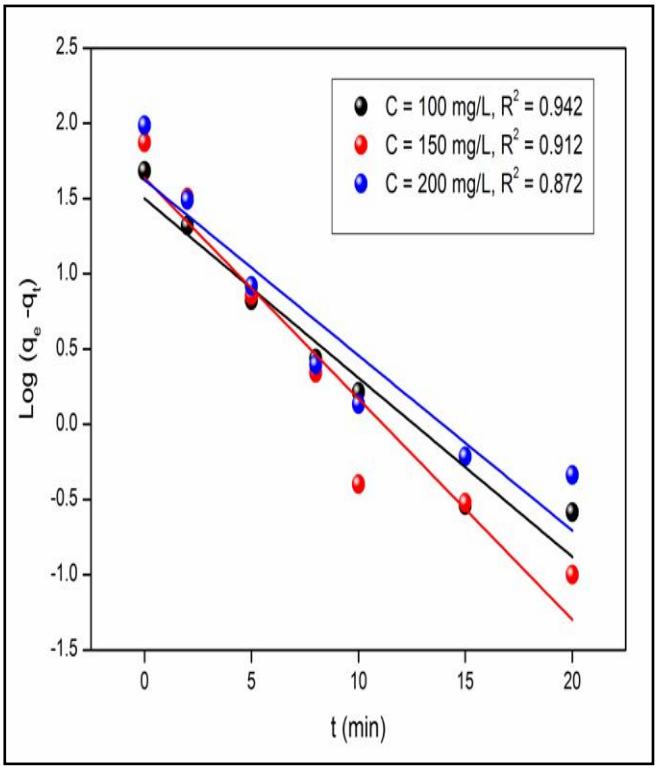


Figure.12: Modeling of the Effect of temperature on the adsorption of BF onto AC

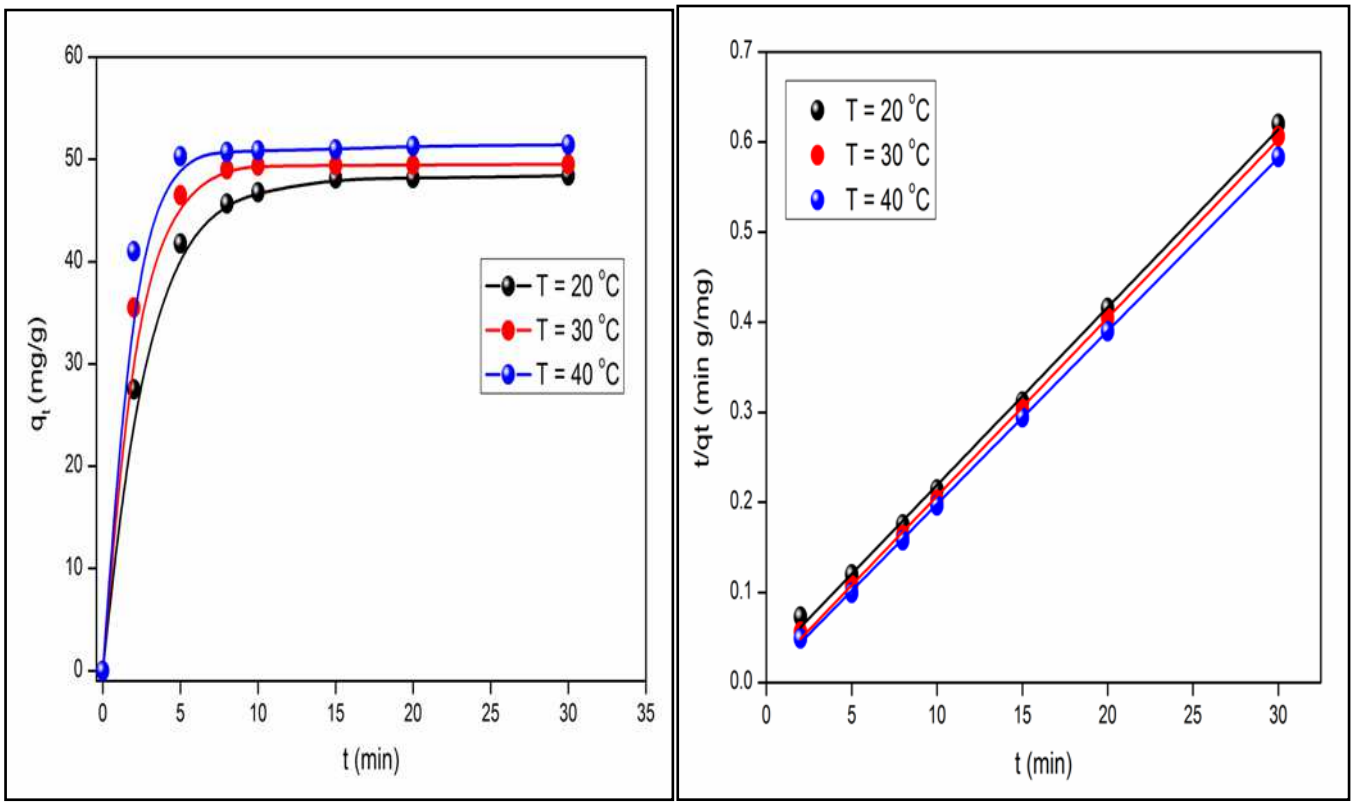


Figure.13: Regression of the thermodynamic parameters of BF adsorption onto AC

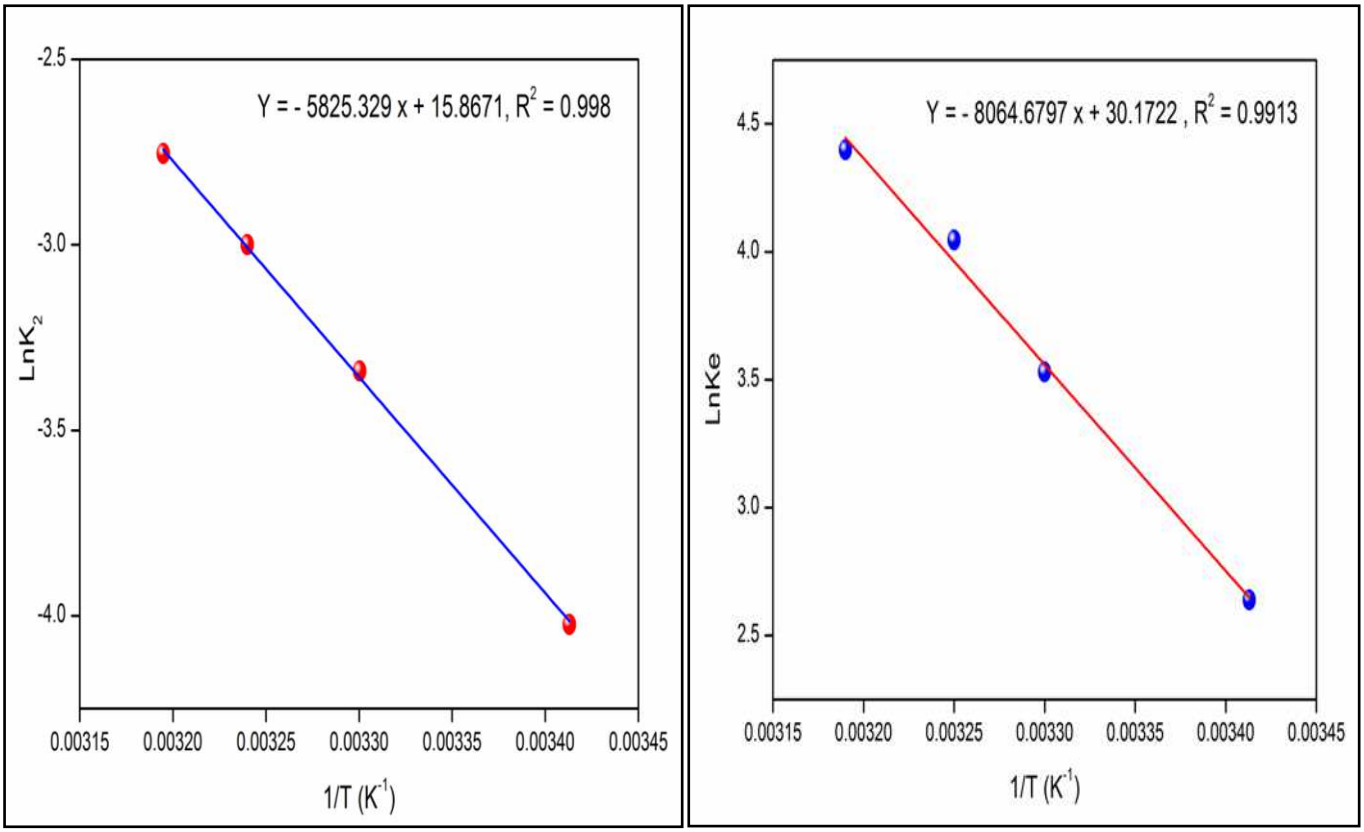


Figure.14: Probable mechanism for BF adsorption onto AC

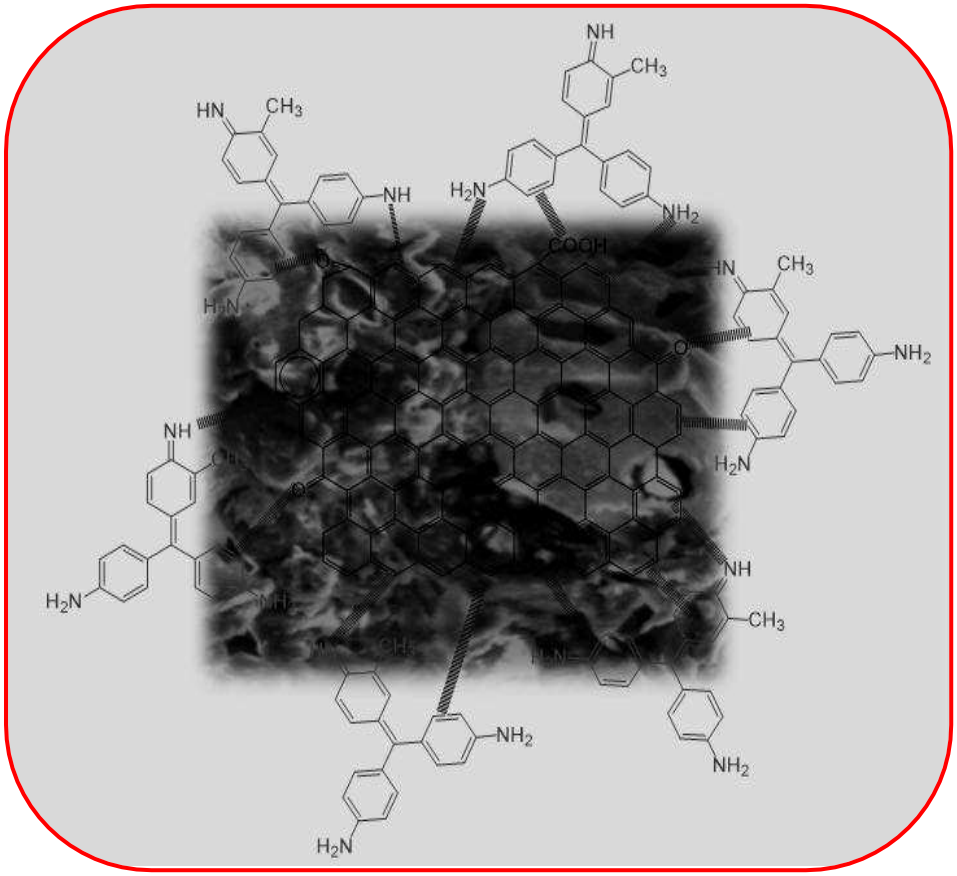


Figure.15: Phytotoxycity Tests

